

1 **BASEMENT-COVER RELATIONSHIPS AND DEFORMATION IN THE**
2 **NORTHERN PARAGUAI BELT, CENTRAL BRAZIL: IMPLICATIONS FOR THE**
3 **NEOPROTEROZOIC-EARLY PALAEOZOIC HISTORY OF WESTERN**
4 **GONDWANA**

5 Iara Maria dos Santos^{a*}, Roberto Vizeu L. Pinheiro^a, Robert E.
6 Holdsworth^b, Afonso Cesar R. Nogueira^a, Hudson Pereira Santos^a, Fabio
7 Henrique G. Domingos^a.

8
9 ^{a*}Universidade Federal do Pará, Instituto de Geociências, Faculdade de
10 Geologia, CP 1611, 66075-900, Belém PA, Brazil.

11 ^bDepartment of Earth Sciences, Durham University, Sciences Labs,
12 Durham DH13LE, UK.

13
14 *Corresponding author: (iarageo13@gmail.com) Iara Maria dos Santos
15
16
17
18
19
20
21
22
23
24

ABSTRACT

25
26 The Northern Paraguai Belt, at the SE border of the Amazonian Craton,
27 central Brazil, has been interpreted as a Brasiliano/Pan-African (ca. 650-
28 600 Ma) belt with a foreland basin, recording collisional polyphase
29 tectonism and greenschist facies metamorphism extending from the late
30 Precambrian to the Cambrian-Ordovician. New structural investigations
31 indicate that the older metasedimentary rocks of the Cuiabá Group
32 represent a Tonian-Cryogenian basement assemblage deformed in two
33 contemporaneous fault-bounded structural sub-domains of wrench-
34 (rake $<10^{\circ}$) and contraction- (rake $\sim 30-40^{\circ}$) dominated sinistral
35 transpression, with tectonic vergence towards the SE. The younger late-
36 Cryogenian to early-Cambrian sedimentary rocks lying to the NW of the
37 Cuiabá Group are non-metamorphic and display only pervasive brittle
38 transtension characterized by normal-oblique faults, fractures and forced
39 drag folds with no consistent vergence pattern. Our analyses suggest that
40 an unconformity separates the metasedimentary Cuiabá Group basement
41 of the Northern Paraguai Belt from the unmetamorphosed sedimentary
42 cover. It is proposed that the latter units were deposited during a post-
43 glacial marine transgression (after ca. 635 Ma) in a post-collisional basin.
44 The Paraguai Belt basement and its post-collisional sedimentary cover
45 share a number of significant geological similarities with sequences in the
46 Bassarides Belt and Taoudéni Basin in the SW portion of the West African
47 Craton.

48

49 **Keywords:** WESTERN GONDWANA; BRASILIANO/PAN-AFRICAN
50 OROGENY; AMAZONIAN CRATON; NORTHERN PARAGUAI BELT.

51

52 The rifting and breakup of Rodinia during the Mesoproterozoic to early
53 Neoproterozoic were associated with the deposition of thick marine
54 siliciclastic rocks along newly formed continental margins, as observed in
55 the Northern Paraguai Belt along the southern border of the Amazonian
56 Craton, central Brazil (Tokashiki & Saes 2008). Later, during the assembly
57 of Gondwana and closure of the Pharusian-Goiás ocean (ca. 660-650 Ma),
58 these rocks were deformed and underwent low grade metamorphism
59 (Alvarenga & Trompette 1993; Cordani *et al.* 2013). Evidence for this
60 continental collisional event is well preserved in both the South American
61 and African continents (Almeida 1984; Trompette 1994; Trindade *et al.*
62 2006; Tohver *et al.* 2006, 2010; Nogueira *et al.* 2007; Alvarenga *et al.*
63 2012; Bandeira *et al.* 2012; Cordani *et al.* 2013; McGee *et al.* 2015;
64 Merdith *et al.* 2017).

65 In South America, the deformed Tonian-Cryogenian rocks of the
66 Northern Paraguai fold-thrust belt are known also to be associated with
67 late-Cryogenian to Early Cambrian rocks that outcrop in the southern
68 region of the Amazonian Craton; these have been previously interpreted
69 as being part of a related foreland basin sequence (Alvarenga *et al.* 2012;
70 McGee *et al.* 2014, 2015; Fig. 1).

71 In the Northern Paraguai Belt, the tectonic deformation of both
72 metasedimentary and adjacent supposedly foreland sedimentary

73 successions are interpreted by Almeida (1964a,b; 1984), Luz *et al.*
74 (1980), Alvarenga & Trompette (1993), Costa *et al.* (2015) and
75 Vasconcelos *et al.* (2015) to be a result of polyphase tectonism. At least
76 four deformation phases, marked by sets of thrust-faults, folds and
77 cleavages, are recognized and related to the long-term collisional history
78 of this orogen that contributed to the assembly of Gondwana at this time
79 (e.g. Alvarenga & Trompette 1993). Importantly, there is no evidence of
80 metamorphism in the younger sedimentary rocks of the supposed
81 foreland basin sequence since organic matter is preserved as a common
82 rock component (Nogueira & Riccomini 2006; Brelaz 2012; Milhomem
83 Neto *et al.* 2013).

84 The present study brings new field data and structural
85 interpretations concerning the regional setting and significance of the
86 rocks exposed along the so-called Northern Paraguai Belt (location A in
87 Fig.1). The newly acquired data are linked to the available regional
88 geological information and the geological sequences are also compared
89 with similar rock sequences preserved along strike in West Africa. The
90 ultimate aim here is to better understand the Neoproterozoic to Cambrian
91 evolution of this important part of the western Gondwana.

92

93

94

95

96

97 REGIONAL GEOLOGY

98 STRATIGRAPHY

99 The Northern Paraguai Belt is part of an important orogen related to the
100 assembly of Gondwana that lies along the southern limit of the Amazonian
101 Craton in central South America (Fig. 1). It is classically described as a
102 fold and thrust belt with a supposedly adjacent foreland basin located
103 immediately to the north and west (e.g. Almeida 1984; Alvarenga &
104 Trompette 1993; Nogueira *et al.* 2007; McGee *et al.* 2014, 2015). The
105 belt comprises older Tonian-Cryogenian metasedimentary rocks of the
106 *Cuiabá Group* and younger Marinoan glacial deposits of the *Puga*
107 *Formation*, Ediacaran limestones of the *Araras Group* and Cambrian-
108 Ordovician siliciclastic rocks of the *Alto Paraguai Group* (Fig. 2; Fig. 3;
109 Almeida 1964, 1984; Trompette 1994; Nogueira *et al.* 2003; Alvarenga *et*
110 *al.* 2004, 2012; Nogueira & Riccomini 2006; Nogueira *et al.* 2007; Tohver
111 *et al.* 2010, 2011; Bandeira *et al.* 2012; McGee *et al.* 2014, 2015; Santos
112 *et al.* 2017; Nogueira *et al.* 2019).

113 The rocks of the Cuiabá Group (Almeida 1964, 1965) are turbiditic
114 siliciclastic successions, deposited in a platformal setting, during early
115 Neoproterozoic rifting of the Rodinia Supercontinent at about 1.2-0.8 Ga
116 (Tokashiki & Saes 2008; Babinski *et al.* 2018). Sm/Nd whole-rock ages
117 obtained in an attempt to elucidate the source-area for the Cuiabá Group
118 rocks yield ages of 0.9-2.1 Ga (Babinski *et al.* 2018). According to these
119 data, the rocks of the Amazonian Craton represent the main source area
120 for the Cuiabá Group. These rocks underwent ductile deformation and

121 greenschist facies metamorphism (Tokashiki & Saes 2008) and Ar/Ar
122 cooling ages of 541 ± 10 to 484 ± 12 Ma have been obtained in these
123 sequences (Geraldes *et al.* 2008; Tohver *et al.* 2010). Dating of ultramafic
124 bodies intruded into the Cuiabá Group rocks, exposed in the Planalto da
125 Serra region, have yielded an intrusion age of about 600 Ma (Rb/Sr and
126 K-Ar; De Min *et al.* 2013).

127 Records of marine transgressions along the glacial platform during
128 the Cryogenian/Ediacaran are thought to be related to the end of the
129 Marinoan Glaciation, around 635 Ma ago (Kirschvink *et al.* 1997; Hoffman
130 & Schrag 2002; Nogueira *et al.* 2003). The rocks of the Puga Formation
131 are tillites with striated pebbles of sandstone, gneiss and granitic rocks,
132 interpreted as Marinoan deposits (706 ± 9 Ma U/Pb detrital zircon; Babinski
133 *et al.* 2013) related to a glacially influenced platformal environment
134 (Maciel 1959; Almeida 1964a, b; Alvarenga & Trompette 1992; Nogueira
135 *et al.* 2003).

136 The Ediacaran Araras Group comprises four units: the Cap
137 Dolostones of the *Mirassol d'Oeste Formation*, interpreted as part of a
138 shallow marine platform; the *Guia Formation* representing limestones and
139 bituminous shales interpreted as deep platformal deposits; the *Serra do*
140 *Quilombo Formation*, which includes dolostones and dolomitic breccias
141 associated with moderately deep to shallow platformal conditions and the
142 *Nobres Formation* comprising dolomites, cherts, sandstones, carbonatic
143 shales formed in a peri-tidal environment (Nogueira & Riccomini 2006;
144 Brelaz 2012; Milhomem Neto *et al.* 2013). The maximum depositional

145 ages of the rocks of the Mirassol d'Oeste and Guia formations are
146 respectively provided by U/Pb detrital zircon ages and Pb/Pb whole rock
147 ages in the range 627 ± 32 to 622 ± 33 (Babinski *et al.* 2006; Romero *et al.*
148 2013) and a U/Pb detrital zircon of 652 ± 5 (Babinski *et al.* 2018). None of
149 these rocks show any clear evidence of regional metamorphism, with
150 organic matter widely preserved in the rocks of the Guia and Serra do
151 Quilombo formations (Nogueira & Riccomini 2006; Brelaz 2012;
152 Milhomem *et al.* 2013).

153 The western and northern segments of the Northern Paraguai Belt
154 (Figs. 2 and 3) are also associated with siliciclastic rocks of the Alto
155 Paraguai Group, which comprise Cambrian to Ordovician siliciclastic
156 deposits including conglomerates, sandstones and shales interpreted as
157 platformal sediments influenced by storms, waves and tides, grading up
158 into the fluvial-lacustrine systems (Almeida 1964; Alvarenga & Saes
159 1992; Bandeira *et al.* 2007, 2012; Santos *et al.* 2017). The maximum
160 depositional ages of the upper succession of the Alto Paraguai Group
161 obtained by Ar/Ar (detrital muscovite) and U/Pb (detrital zircon) are 622
162 Ma and 544 Ma - 541 Ma, respectively (Bandeira *et al.* 2012; McGee *et al.*
163 2014, 2015). Records of *Skolithos* ichnofacies burrows in the rocks of the
164 lowermost Alto Paraguai Group suggest a Lowermost Cambrian age or
165 younger for these rocks (Santos *et al.* 2017).

166 All of the post-Cryogenian deposits have been interpreted as
167 foredeep sediments laid down in a major foreland basin related to the
168 Northern Paraguai Belt (Alvarenga *et al.* 2004; Nogueira *et al.* 2007;

169 Tohver *et al.* 2010 and 2011; Bandeira *et al.* 2012; McGee *et al.* 2014,
170 2015). A recently proposed alternative interpretation suggest that they
171 represent an intracratonic basin sequence formed in the southern portion
172 of the Amazonian Craton and related to eustatic transgressions that
173 occurred during the Ediacaran-Cambrian (Nogueira *et al.* 2019).

174 The São Vicente Granite, dated at 518 ± 4 Ma (U/Pb zircon; McGee *et*
175 *al.* 2012), and the Mesozoic basalts of the Tapirapuã Formation, locally
176 cut and post-date the rocks of Paraguai Belt (Montes-Lauar *et al.* 1994).
177 Most of the Neoproterozoic/Cambrian rocks of the Cuiabá Group, the Puga
178 Formation, the Araras and Alto Paraguai groups are also unconformably
179 overlain by post-Ordovician sedimentary rocks of the Paraná and Parecis
180 basins (Figs. 2; Fig. 3).

181

182 *REGIONAL TECTONIC CONTEXT*

183 The deformation of the Northern Paraguai Belt is thought to be related to
184 the Brasiliano/Pan-African Orogeny, and has been described as a
185 polyphase event that decreases progressively in intensity and
186 metamorphic grade from E to W, towards the Amazonian Craton (Fig 1;
187 Almeida 1964, 1984; Almeida & Hasui 1984; Alvarenga & Trompette
188 1993). It has been classically subdivided into three major structural
189 domains in order to explain its deformation patterns and tectonic
190 evolution (Almeida 1964, 1984; Alvarenga & Trompette 1993): an
191 *Internal Zone* comprising metasedimentary rocks of the Cuiabá Group,
192 mainly deformed by folds, thrust-faults and associated cleavages; an

193 *External Zone* including little metamorphosed sedimentary rocks of the
194 Puga Formation, Araras and Alto Paraguai groups, also deformed by folds,
195 sub-vertical thrust-faults and cleavage; and a *Platform Sedimentary*
196 *Cover* which represents the same sequence of sedimentary rocks that are
197 only weakly deformed.

198 Four deformation phases have been proposed to affect the rocks of
199 the Northern Paraguai Belt (Luz *et al.* 1980; Souza 1981; Pires *et al.*
200 1986; Alvarenga 1986, 1990; Del'Rey Silva 1990; Alvarenga & Trompette
201 1993; Silva 1999; Silva *et al.* 2002; Costa *et al.* 2015; Vasconcelos *et al.*
202 2015). The first phase (D1) is thought to be responsible for the main
203 deformation of rocks of the Cuiabá Group, exposed in the Internal Zone
204 as isoclinal to tight folding, with an associated NE-SW trending cleavage
205 (S1) and NE-SW reverse faults. The second (D2) and third deformation
206 phases (D3) are thought to affect rocks in both the Internal and External
207 zones, and are marked by the development of crenulation cleavages, NE-
208 SW and NW-SE fractures, as well as open folds. A fourth deformation
209 phase (D4) is mainly represented by fractures oriented perpendicularly to
210 the main foliation trend, found in the sedimentary rocks of the External
211 Zone.

212 The tectonic vergence of the belt is thought by some authors to be
213 towards the NW (Almeida 1964, 1984; Nogueira & Oliveira 1978; Corrêa
214 *et al.* 1979; Alvarenga 1986, 1990; and McGee *et al.* 2014, 2015),
215 although Luz *et al.* (1980), Alvarenga & Trompette (1993), Costa *et al.*
216 (2015) and Vasconcelos *et al.* (2015) propose an opposite southeastward

217 vergence. Silva (1999) has suggested a model involving the presence of
218 back-thrusts in order to explain the possibility of two contemporaneous
219 and opposed tectonic vergence directions.

220 **FIELD DATA - STRUCTURAL ANALYSES**

221 The tectonic structures and the rocks of the Northern Paraguai Belt and
222 its adjacent sedimentary cover are well exposed in road cuts and natural
223 outcrops between Cuiabá, Guia, Poconé, Planalto da Serra, Nobres,
224 Diamantino, Cáceres and Mirassol d'Oeste (Mato Grosso State) (Fig. 3).
225 The three-dimensional geometry, inter-relationships and kinematics of the
226 structures preserved, are illustrated in supported by field observations
227 and structural data.

228 Geometric and kinematic analyses show that the complex,
229 seemingly polyphase structures of the Northern Paraguai Belt are more
230 simply interpreted in terms of progressive deformation and partitioning
231 during two successive transpressional-transtensional episodes (following
232 the concepts and models of Fossen *et al.* 1994; Dewey *et al.* 1998; Tikoff
233 & Fossen 1999; Holdsworth *et al.* 2002; Jones *et al.* 2004; Fossen *et al.*
234 2018 for example). As shown in the following sections, the
235 metasedimentary rocks of the Cuiabá Group have been deformed during a
236 single episode of ductile transpression forming the 'Transpressional
237 Structural Domain' (TPSD), whilst the younger sedimentary rocks of the
238 Puga Formation and Araras-Alto Paraguai groups are affected by brittle
239 transtensional deformation (Fig. 3) forming a later 'Transtensional
240 Structural Domain' (TTSD). The younger brittle transtensional structures

241 are also widely recognized locally overprinting the ductile TPSD structures
242 in the Cuiabá Group.

243

244 *TRANSPRESSIONAL STRUCTURAL DOMAIN (TPSD)*

245

246 The rocks deformed by transpression outcrop mainly in the southeastern
247 part of the surveyed region (Fig 3). They correspond to phyllites,
248 metapelites, metaconglomerates and metasandstones of the Cuiabá
249 Group (Fig. 4). The ductile to brittle-ductile deformation of these
250 metasedimentary rocks forms a series of NE-SW and E-W-trending
251 foliated domains (Fig. 3; Fig. 4). Fine continuous foliations (in phyllites)
252 and spaced foliations (in the metapelites, metasandstones and
253 metaconglomerates) are developed everywhere, both of which carry
254 stretching lineations (Fig. 4; Figs. 5B, 5C, 5E). Compositional layering
255 thought to correspond to bedding is preserved in less deformed regions
256 (e.g. Fig. 5A). Regional to mesoscopic folds are observed deforming both
257 the bedding and, locally, the continuous foliations (Fig. 3; Figs. 5A, 5B).

258 A regional-scale anastomosing network of higher strain NE-SW
259 sinistral transpressional shear zones is recognized associated with
260 sinistrally verging asymmetric folds. Two structural sub-domains sharing
261 the same regional foliation can be defined based on the angular
262 relationships between foliations and lineations (rake) in the shear zones.
263 These reveal two quite distinct kinematic domains: (1) those with
264 moderate lineation rake angles (typically ca. 30° to 40°); and (2) those

265 with low rake angles ($<10^\circ$), referred to here as TPSD-A and TPSD-B,
266 respectively. The mapped extent of these structural domains is shown in
267 Figure 3. Given the common regional foliation and ubiquitous sinistral
268 vergence of associated minor structures, these are interpreted in terms of
269 a partitioned transpressional deformation in the rocks of the Cuiabá Group
270 with a regional vergence direction towards the SE.

271 The rocks of the TPSD-A sub-domain are mostly low-grade
272 metasedimentary rocks that display bedding planes with NE-SW strikes
273 and steep to gentle dips towards both the NW and SE (Figs. 5A, 5B).
274 Recumbent to moderately reclined folds of bedding are common, with NE-
275 SW axial planes and gentle plunging SW β axis; vergence overall is to the
276 SE (Fig. 5A). Sets of tens-to-hundred-meter wide NE-SW shear zones cut
277 across these rocks, developing a fine continuous foliation in metapelites,
278 with gentle to moderate dips towards NW and SE (Fig. 5B; Fig. 6).
279 Stretching lineations associated with this continuous foliation are
280 shallowly plunging towards the N, NW and NE, with typical rake angles of
281 $30-40^\circ$ (Fig. 5C; Fig. 6A). The fine continuous foliation is itself deformed
282 by asymmetric moderately reclined folds indicating sinistral kinematics,
283 with axial planes striking NE-SW, and a regional β axis plunging gently
284 NE, with a southeastward vergence direction (Fig.3; Fig. 5A). Oblique
285 thrust-faults are observed both in regional and outcrop scales, with NE-
286 SW strike and low angle dips towards the NW approaching sub-horizontal
287 (Fig. 3; Fig. 5C; Fig. 6A). The inclined regional foliation, moderately
288 plunging mineral lineations and associated sinistral shear criteria are

289 consistent with an inclined transpressional deformation, possibly
290 contraction-dominated (see for example Holdsworth *et al.* 2002; Jones *et*
291 *al.* 2004)

292 The TPSD-B sub-domain (Fig.3; Fig.5) is characterized by much
293 more highly deformed metasedimentary rocks in shear zones and shear
294 bands, with a NE-SW anastomosing mylonitic foliation showing steep to
295 sub-vertical dips towards NW and SE (Fig. 5D; Fig. 6C). Stretching
296 lineations plunge consistently gently to the NE and SW, with a 10°
297 average rake angle (Fig. 5E). The fine continuous foliation may show local
298 transposition along shear bands, and sinistral asymmetric drag folds (Fig.
299 6C). The steep dips of the foliation with shallowly plunging associated
300 mineral lineations and sinistral shear criteria suggest a wrench-dominated
301 transpressional strain pattern (see for example Holdsworth *et al.* 2002;
302 Jones *et al.* 2004).

303 Under the microscope, the fine grained metapelites of the Cuiabá
304 Group in both sub-domains show fine grained spaced foliation defined by
305 the aligned arrangement of muscovite, ribbons and aggregates of quartz
306 and feldspar grains (Fig. 7). Aggregates of quartz and K-feldspar locally
307 display discrete sinistral asymmetry (Figs. 7A, 7B). A set of conjugate
308 crenulation cleavages (Fig. 8) with centimeter-scale spacing, show NE-SW
309 and NW-SE strikes with gentle dips towards NW and SE and steep dips
310 towards NE; vergence senses associated with this cleavage show
311 consistent dextral asymmetry (Fig. 8B; Fig. 9A).

312 The fine continuous fabrics that dominate in the rocks of the Cuiabá
313 Group are everywhere cut by sets of NW-SE, N-S, ENE-WSW and NE-SW
314 sets of normal-oblique faults and fractures (Fig. 9B). Tabular quartz veins
315 are found in metasandstones, metaconglomerates and phyllites of the
316 Cuiabá Group. They range from a few millimeters to a few meters thick
317 and lie parallel, subparallel, or discordant to the foliation of the
318 metasedimentary rocks in the TPSD (Fig. 4C). They are NE-SW, NW-SE,
319 N-S and E-W striking, with moderate to sub-vertical dips towards the NW,
320 SW, NE and S, respectively (Fig. 9C). They are thought to be associated
321 with the late normal-oblique faults and fractures. Some of these veins
322 host important gold deposits, and are locally mined (Tokashiki & Saes
323 2008; Vasconcelos *et al.* 2015).

324 *TRANSTENSIONAL STRUCTURAL DOMAIN (TTSD)*

325 The sedimentary rocks of the Puga Formation, Araras Group and Alto
326 Paraguai Group include pelites, tillites, dolostones, calcitic shale,
327 sandstones and shales (Fig. 2; Fig. 10), which are juxtaposed by normal
328 faulting against the rocks of Cuiabá Group to the southeast (Fig. 3).
329 Deformation here is characterized by normal-oblique faults, drag folds,
330 fractures/joints, and locally developed cataclastic foliations (Figs. 11; Fig.
331 15).

332 The main sets of normal-oblique and strike-slip faults observed in
333 the sedimentary rocks trend NE-SW, NW-SE, N-S and E-W (Fig. 11C, 11I,
334 11N). The NE-SW normal-oblique faults have steep to sub-vertical planes,
335 dipping towards the NW and SE, with shallowly SW plunging oblique

336 striations showing NW-side down, sinistral kinematics (Figs. 11D, 11F,
337 11I, 11J, 11N, 11O). The NW-SE normal-oblique faults also have steep to
338 sub-vertical dips towards SW, and shallowly NW plunging striations
339 showing SE-side down, dextral oblique kinematics (Figs. 11D, 11F, 11I,
340 11J, 11N, 11O). The N-S normal-oblique faults have steep to sub-vertical
341 dips towards E and W, and show down-dip to oblique-dip striations with a
342 shallow northward plunge (Figs. 11D, 11F, 11I, 11J, 11N, 11O). The E-W
343 strike-slip faults show steep to sub-vertical dip angles towards the N and
344 S and show shallowly E or W plunging striations (Figs. 11D, 11F, 11I, 11J,
345 11N, 11O). The asymmetry of the regional and mesoscopic drag folds
346 located near to the NE-SW and NW-SE trending normal oblique faults
347 indicates a mainly dextral sense of shear, suggesting a dextral
348 transtension.

349 The NE-SW, NW-SE and E-W normal-oblique and strike-slip faults,
350 described above, are responsible for local to regional drag folding in the
351 sedimentary rocks (Figs. 11A, 11F, 11K; Fig. 12). Fold axis are
352 moderately to shallowly plunging SE, SW and NE (Figs. 12B, 12C);
353 associated axial planes strike NE-SW with steep dips towards NW, as well
354 as NW-SE with moderate to steep dips towards the NE (Fig. 11B, 11G,
355 11L). These fault-related folds are moderately reclined to upright, open to
356 tight, with variable vergence towards either the SW or SE; the overall
357 asymmetries of the brittle mesoscopic drag folds are consistent with
358 regional dextral kinematics (Figs. 11A, 11F, 11K; Fig. 12).

359 A cataclastic foliation cuts both metasedimentary rocks of the TPSD
360 and the sedimentary rocks of the TTSD and is closely related to the
361 presence of the normal-oblique and strike-slip faults and fractures and
362 associated folds (Fig. 12). It shows mainly N-S to NNE-SSW strikes, with
363 moderate to sub-vertical dips towards the SE (Fig. 11E). This non-
364 penetrative foliation develops in tens to hundreds of meters wide
365 corridors that are hundreds of meters to kilometers long in map view. It is
366 found in all rocks of the Northern Paraguai Belt and is an anastomosing
367 foliation that locally transposes all earlier structures (Fig. 6C; Fig. 12).

368 A notably large set of folds is observed near the Nossa Senhora da
369 Guia city (Fig.3; Fig. 13), north of Cuiabá and corresponds to a ca. 20 km
370 long and ca. 3 km wide synclinal structure deforming calcitic shales and
371 limestones of the Guia Formation (Nogueira & Riccomini 2006; Brelaz
372 2012), and faulted against the Cuiabá Group metasedimentary rocks. This
373 large fold has been attributed by Almeida (1964, 1984), Luz *et al.* (1980)
374 and Alvarenga & Trompette (1993) to the effects of the Brasiliano/Pan-
375 African Orogeny affecting the younger sedimentary rocks in the region.

376 Our field observations show that near the borders of the syncline,
377 the metapelites of the Cuiabá Group have developed a pervasive NE-SW
378 continuous foliation dipping 55°-60° towards the NW (Fig. 14). These
379 rocks form part of the TPSD-A sub-domain (Fig. 3). The major syncline -
380 defined by folded and faulted bedding is developed in limestones of the
381 younger Guia Formation rocks that are inferred, based on their
382 unmetamorphosed state, to have originally unconformably overlain the

383 metasedimentary rocks of the Cuiabá Group. The bedding inside the
384 syncline is mostly flat, and is only folded and rotated into steep 65° - 85°
385 NW dips adjacent to the bounding normal fault. Fold hinges are parallel to
386 the NE-SW normal fault planes, plunging shallowly to sub-horizontally
387 towards the NE and SW (Fig. 13; Fig. 14). The contacts between the
388 sedimentary and metasedimentary rocks are NE-SW normal-oblique fault
389 zones with steep dips (75° - 85°) towards NW and SE (Fig. 13; Fig. 14).

390 **SUMMARY**

391 The exposed metasedimentary rocks of the Cuiabá Group show pervasive
392 effects of ductile deformation in which two structural sub-domains of
393 partitioned transpressional deformation are recognized (Fig. 3). The
394 TPSD-A domain is characterized by shallow to moderately-dipping NE-SW
395 shear zones, fine continuous foliation and stretching lineations with rakes
396 of about 40° , consistent with a sinistral contraction-dominated
397 transpression. The TPSD-B domain has high strain sinistral shear zones
398 with moderately to subvertically dipping mylonitic foliations and shallowly
399 plunging stretching lineations (rakes around 10°), suggesting a wrench-
400 dominated transpression. The rocks related to both structural sub-
401 domains share the same regional foliation and show a consistent tectonic
402 vergence towards the SE. Metamorphism is low to medium greenschist
403 facies (Tokashiki & Saes 2008).

404 The late-Cryogenian to Cambrian rocks of the Puga Formation,
405 Araras and Alto Paraguai groups, exposed in the northern and western

406 region of the Northern Paraguai Belt, have not experienced regional
407 metamorphism (Nogueira & Riccomini 2006; Brelaz 2012; Milhomem Neto
408 *et al.* 2013) and show no ductile transpressional deformation.
409 Deformation in these younger sedimentary sequences is marked by brittle
410 oblique-slip faults and shear zones in a range of orientations with
411 cataclastic foliations locally developed. Folds are present here, but are
412 interpreted to be normal oblique faults-related drag structures. The folds
413 are drag or strike-slip-related features as are found in other
414 transtensional settings (e.g. De Paola *et al.* 2005). These are asymmetric,
415 moderately inclined to upright and show no consistent vergence pattern.
416 These structures are consistently found adjacent to NE-SW normal oblique
417 faults suggesting that they were formed during transtensional regional
418 deformation in the TTSD.

419 The rocks of Cuiabá Group locally display NE-SW, NW-SE, N-S and
420 E-W-trending zones of late dextral crenulation cleavage, which transects
421 the older fine continuous foliations. This cleavage is developed sub-
422 parallel to the TTSD brittle features and is interpreted to represent zones
423 of overprinting grain-scale brittle deformation developed preferentially in
424 mica-rich metasedimentary rocks.

425

426

427

428 **DISCUSSION**429 *THE AGES OF BASEMENT AND COVER*

430 The Brasiliano/Pan-African Orogeny is generally related to the tectonic
431 assembly of the western Gondwana. This event is thought to be
432 responsible for the deformation and metamorphism of the Cuiabá Group
433 rocks in the Northern Paraguai Belt (Fig.3).

434 De Min *et al.* (2013) used K/Ar, Ar/Ar and Rb/Sr geochronology to
435 suggest an age of 600 Ma for the intrusion of ultramafic bodies into the
436 Cuiabá Group, and Babinski *et al.* (2018) have obtained a U-Pb detrital
437 zircon age of 652 ± 5 Ma for the calcitic limestones of the Guia Formation.
438 Importantly, our findings suggest that the Guia Formation should be
439 included in the Araras Group, and that it is *not* part of the Northern
440 Paraguai Belt basement. These rocks show neither metamorphism or
441 transpressional ductile deformation, contrary to previously suggestions
442 made by Luz *et al.* (1980), Tokashiki & Saes (2008) and McGee *et al.*
443 (2015). This implies that both the Cuiabá Group and its associated
444 transpressional ductile deformation and metamorphism are *older* than
445 652-600 Ma. Thus, there is no field or other evidence to support the idea
446 that Brasiliano/Pan-African metamorphism and ductile deformation
447 continued into the Cambrian-Ordovician.

448 Based on our structural observations in the field and thin section,
449 we suggest that the Cambrian-Ordovician Ar/Ar cooling ages recorded by
450 the Cuiabá Group (Geraldés *et al.* 2008; Tohver *et al.* 2010) are most

451 likely related to post-collisional overprinting. This could very well be
452 related to the development of the transtensional faults and associated
453 drag folds which are found both in the Neoproterozoic metasedimentary
454 rocks and in the Ediacaran to early Cambrian sedimentary cover
455 sequences.

456 *IS A FORELAND BASIN PRESENT?*

457 Luz *et al.* (1980), Almeida *et al.* (1984), Alvarenga & Trompette (1993),
458 Nogueira *et al.* (2007) Alvarenga *et al.* (2012), Bandeira *et al.* 2012 and
459 McGee *et al.* (2014, 2015) have argued that the rocks of the Cuiabá
460 Group, Puga Formation, Araras and Alto Paraguai groups represent a fold
461 and thrust and foreland-foredeep system in which the tectonic
462 deformation was driven by the continuous shortening of the adjacent
463 orogen.

464 A foreland basin typically is related to down-flexure of the
465 lithosphere in response to an orogenic load advancing towards the
466 foreland in the direction of tectonic vergence (DeCelles *et al.* 2002).
467 According to Almeida (1964, 1984), Nogueira & Oliveira (1978), and
468 Corrêa *et al.* (1979), Alvarenga (1986, 1990) and McGee *et al.* (2014,
469 2015). This would require the orogenic vergence to be from the SE
470 towards the NW. Conversely, Luz *et al.* (1980), Alvarenga & Trompette
471 (1993), Costa *et al.* (2015) and Vasconcelos *et al.* (2015) suggest that
472 the vergence was from NW towards the SE. Our structural mapping
473 confirms that the sinistral partitioned transpressional deformation (i.e. the

474 TPSD), developed in the metamorphic rocks of the Cuiabá Group, has a
475 consistent SE vergence (e.g. Fig. 3; Fig. 5; Fig. 6). This would require
476 that any foreland sedimentary succession should lie to the southeast of
477 the collisional belt, not to the northwest, i.e. if present, it would lie below
478 the rocks of the younger Paraná Basin.

479 Previous stratigraphic investigations (Alvarenga & Saes 1992;
480 Nogueira *et al.* 2003; Alvarenga *et al.* 2012; Nogueira & Riccomini 2006;
481 Bandeira *et al.* 2012; Santos *et al.* 2017; Nogueira *et al.* 2019) show that
482 the thick sedimentary cover of the Puga Formation and Araras and Alto
483 Paraguai groups are a succession of glacially influenced deep to shallow
484 marine platform influenced by storms, tides and waves grading up to
485 lacustrine-fluvial system. Well preserved Silurian to Neogene foreland
486 basins (like those found adjacent to the Pyrenees, Alpine-Himalayan
487 system, the Zagros, North Caucasus, South Urals, Appalachian and Andes
488 thrust belts) typically comprise immature sedimentary rocks normally
489 from fluvial/alluvial-fan to a shallow marine platformal
490 paleoenvironments, showing wedge-shaped stratigraphic sequences and a
491 variety of unconformities due the tectonic instability and rapid subsidence
492 rates (Allen & Allen 1990; DeCelles & Giles 1996; DeCelles *et al.* 2002;
493 Chapman & DeCelles 2015). These rocks generally also show progressive
494 metamorphism and zonation of folds and thrust faults, consistent with the
495 progressive foreland-directed advance of the orogenic wedge (Allen *et al.*
496 1991; Saura *et al.* 2011; Zhang *et al.* 2011; Delgado *et al.* 2012;
497 Mouthereau *et al.* 2014; Roigé *et al.* 2017). None of these characteristics

498 are seen in the Ediacaran-Cambrian sedimentary rocks of the Northern
499 Paraguai Belt.

500 The present structural analyses and previous stratigraphic models
501 (Nogueira *et al.* 2003; Nogueira & Riccomini 2006; Bandeira *et al.* 2012;
502 Santos *et al.* 2017; Nogueira *et al.* 2019) suggest that an unconformity
503 exists between the metasedimentary basement rocks of the Northern
504 Paraguai Belt and the younger unmetamorphosed sedimentary cover
505 sequences. Stratigraphic and sedimentological analyses and the general
506 regional tectonic setting seem more consistent with the cover sequences
507 being part of an intracratonic basin, as suggested by Nogueira *et al.*
508 (2019).

509 *COMPARISONS WITH SIMILAR SEQUENCES IN AFRICA*

510 The Brasiliano/Pan-African Orogeny is also recognized in the western part
511 of the West African Craton (Dalziel 1992; Trompette 1994; Tokashiki &
512 Saes 2008; Deynoux *et al.* 2006; Villeneuve 2008). The Rockelides-
513 Bassarides belts have been correlated with the Araguaia and the Northern
514 Paraguai belts based on similarities in general tectonic setting,
515 lithostratigraphy and geochronology (Fig. 15; Trompette 1994, 1997;
516 Villeneuve & Cornée 1994; Shields *et al.* 2007; Deynoux *et al.* 2006;
517 Villeneuve 2008; Paixão *et al.* 2008).

518 Regionally in the Northern Paraguai Belt, siliciclastic successions,
519 deposited ca. 1.2-0.8 Ga during rifting of Rodinia forming a deep to
520 shallow marine platform, are thought to correspond to the protolith of the

521 Cuiabá Group metasedimentary rocks (Dalziel 1992; Tokashiki & Saes
522 2008; Babinski *et al.* 2018). The metamorphic rocks of the Termesse and
523 Guinguan groups, exposed in the Bassarides Belt in southwestern West
524 African Craton (Fig. 15), are similarly related to platformal basins, and are
525 further constrained by Rb/Sr ages obtained from rhyolites thought to date
526 their emplacement between 1.0-1.05 Ga (Villeneuve 2008). The Termesse
527 and Guinguan groups (Fig. 15B) are metavolcanosedimentary and
528 ultramafic rocks whose metamorphic grade ranges from greenschist to
529 amphibolite, that are locally intruded by granitoids, rhyolite, dacite and
530 basalts. They are widely deformed by recumbent to open folds, schistosity
531 and brittle cleavages (Bassot 1966; Villeneuve 1982, 1984).

532 The Bassarides Belt (Fig. 1) is overlain by a flat-lying Paleozoic
533 sedimentary cover, which is correlated with the cratonic sedimentary
534 rocks of Taoudéni Basin in the central portion of the West African Craton
535 (Fig. 1; Fig. 15). In its lower parts, a sequence of Ediacaran to Cambrian
536 sedimentary rocks (Fig. 15) forms the Mali and Batapa groups which
537 unconformably overlie the Bassarides Belt (Villeneuve 2008). These
538 sedimentary rocks include Marinoan tillites of the Walidiala Formation
539 capped by 1000m of cap dolostones, shales, pelites and sandstones
540 interpreted as having been deposited in a new phase of rifting between
541 610-550 Ma (Deynoux *et al.* 2006).

542 There are obvious similarities between the geological relationships
543 shown by the ductile deformed parts of the Northern Paraguai and

544 Bassarides belts, and their geological relationships to overlying and
545 adjacent Late Cryogenian to Early Cambrian Marinoan tillites, cap
546 dolostones and siliciclastic sedimentary rocks (Fig. 15). This agrees with
547 the suggestions of Shields *et al.* (2007) and Villeneuve (2005, 2008) who
548 pointed out that both the rocks of Bassarides Belt and western Taoudéni
549 Basin show stratigraphic and geochronological similarities to those
550 outcropping in the northern areas of the Araguaia and Northern Paraguai
551 belts, in South America (Fig. 16).

552 **SYNTHESIS & CONCLUSIONS**

553 Regionally in the Northern Paraguai Belt, siliciclastic successions forming
554 the protoliths of the Cuiabá Group basement are thought to have been
555 deposited ca. 1.2-0.8 Ga during rifting of Rodinia forming a deep to
556 shallow marine platform (Fig 16A; Tokashiki & Saes 2008; Babinski *et al.*
557 2018). The structural analyses presented here show that the
558 metasedimentary rocks of the Cuiabá Group were then deformed during
559 Brasiliano/Pan African ductile sinistral partitioned transpression at about
560 652-600 Ma (Fig 16B; De Min *et al.* 2013; Babinski *et al.* 2018). The
561 rocks forming this orogen were then unconformably overlain by late-
562 Cryogenian to Cambrian sedimentary rocks (Puga Formation, Araras and
563 Alto Paraguai groups), possibly during a Marinoan eustatic transgression
564 (Fig 16C) as suggested by Nogueira *et al.* (2019).

565 Both the rocks of the Cuiabá Group and the late-
566 Cryogenian/Cambrian sedimentary cover were later deformed by possibly
567 post-Ordovician brittle transtensional structures. This formed both the

568 dextrally verging crenulation fabric developed in the Cuiabá Group
569 basement rocks and the transtensional deformation seen in the late-
570 Cryogenian/early-Cambrian sedimentary sequences (Fig. 16D). In our
571 view, there is no evidence for the existence of a foreland basin at this
572 time and there is therefore no need to extent the effects of orogenesis
573 into the Cambrian.

574 The model proposed requires the development of a large
575 extensional-transtensional regional basin under the influence of the post-
576 glacial eustatic transgression that took place after the Brasiliano/Pan-
577 African Orogeny and Marinoan Glaciation (e.g. Fig. 16C). The presence of
578 very similar successions in Western Africa may indicate that this formed
579 part of an important regional intracontinental episode of basin formation
580 that took place after the Early Cambrian along large parts of the eastern
581 border of the West African/Amazonian cratons in western Gondwana.

582 Finally, sets of very late ENE-WSW normal faults, found in the rocks
583 of the Northern Paraguai Belt (Fig. 16E), are known to be related to
584 Mesozoic rifting during opening of the Atlantic Ocean (Martinelli 1998).
585 The basalts of the Tapirapuã Formation (Montes-Lauar 1994), exposed in
586 the northwestern region of the Northern Paraguai Belt (Fig. 3), are
587 geochemically analogous to the Jurassic basalts of the Serra Geral
588 Formation, overlying the Paleozoic rocks of the Paraná Basin (Barros *et al.*
589 2007).

590 Overall, this study highlights that events related to the assembly of
591 the Western Gondwana during the Brasiliano/Pan-African Orogeny (ca.
592 650-600 Ma) and later intracontinental thermal subsidence or rifting
593 episodes are well preserved in the Northern Paraguai Belt and can be
594 broadly related to very similar sequences in Africa.

595

596 **Acknowledgments**

597 Fieldwork for this study was supported by GEOCIAM Project, UFPA, Brazil
598 (2014-2015). We are grateful to CAPES for MSc. scholarship to IM dos S,
599 and to Amarildo Salinas Ruiz (UFMT, Brazil) and José Bandeira C. da Silva
600 Jr. (UFPA, Brazil) for providing field assistance. We also are very grateful
601 to Alan Collins and an anonymous reviewer for critical reviews and
602 suggestions that allowed significant improvements to the paper.

603

604

605

606

607

608

609

610

611

612

613

614 REFERENCES

- 615 Allen, P. A. & Allen, J. R. 1990. *Basin Analysis*. Principles & Applications.
616 451. Oxford, London, Edinburgh, Boston, Melbourne: Blackwell
617 Scientific.
- 618 Allen, P.A., Crampton, S.L., & Sinclair, H.D. 1991. The inception and early
619 evolution of the North Alpine foreland basin, Switzerland: *Basin*
620 *Research* **3**, 143–163.
- 621 Almeida, F.F.M. 1964a. Geologia do Centro – Oeste Mato-grossense.
622 *Boletim da Divisão de Geologia e Mineralogia*. **53**.- DNPM, Ministério
623 das Minas e Energia, Rio de Janeiro.
- 624 Almeida, F.F.M., 1964b. Glaciação Eocambriana em Mato Grosso, Brasil.
625 *Ministério das Minas e Energia*. DNPM. Early notes. Est. **117**, 1–10.
- 626 Almeida, F.F.M. 1965. Geologia da Serra da Bodoquena (Mato- Grosso).
627 **96**. *Boletim da Divisão de Geologia e Mineralogia* - DNPM, Ministério
628 das Minas e Energia, Rio de Janeiro **230**, 1-100.
- 629 Almeida, F.F.M. 1984. Província Tocantins, setor Sudoeste. In: Almeida,
630 F.F.M. and Hasui, Y. (Eds) 1984. *O Pré-Cambriano do Brasil*. São Paulo:
631 Blücher, 265–281.
- 632 Alvarenga, C.J.S. 1986. Evolução das Deformações Polifásicas Brasilianas
633 na Faixa Paraguai, região de Cuiabá, MT. *Anais do Congresso Brasileiro*
634 *de Geologia*, **34**. Goiânia. SBG. **3**, 1170-1175.
- 635 Alvarenga, C.J.S., 1990. Phénomènes sédimentaires, structuraux et
636 circulation de fluides à la transition Chaîne-Craton: Exemple de la cote
637 Paraguai d'âge Proterozoïque Supérieur. PhD thesis. University of
638 Marseille 3, Mato Grosso, Brésil.
- 639 Alvarenga, C.J.S. & Trompette, R. 1992. Glacially influenced
640 sedimentation in the later Proterozoic of the Paraguai Belt (Mato
641 Grosso, Brazil). *Palaeogeografia, Palaeoclimatologia, Palaeoecologia* **92**,
642 85-105.
- 643 Alvarenga, C.J.S. & Saes, G.S. 1992. Estratigrafia e sedimentologia do
644 Proterozóico Médio e Superior da região sudeste do Cráton
645 Amazônico. *Brazilian Journal of Geology*, **22**(4), 493-499.
- 646 Alvarenga, C.J.S. & Trompette, R. 1993. Evolução Tectônica Brasileira da
647 Faixa Paraguay: a Estruturação da Região de Cuiabá. *Brazilian Journal*
648 *of Geology* **23** (1), 18-30.
- 649 Alvarenga, C.J.S., Santos, R.V. & Dantas, E.L. 2004. C–O–Sr Isotopic
650 Stratigraphy of Cap Carbonates Overlying Marinoan-age Glacial
651 Diamictites in the Paraguay Belt, Brazil. *Precambrian Research* **131**, 1–
652 21.
- 653 Alvarenga, C.J.S., Boggiani, P. C., Babinski, M., Dardenne, M. A.,
654 Figueiredo, M. F., Dantas, E. L., Uhlein, A., Santos, R.V., Sial, A. N. &

- 655 Trompette, R. 2012. Glacially influenced sedimentation of the Puga
656 Formation, Cuiabá Group and Jacadigo Group, and associated
657 carbonates of the Araras and Corumbá groups, Paraguay Belt, Brazil.
658 *Geological Society, London, Memoirs* **36**, 487-497.
- 659 Babinski, M., Trindade, R.I.F., Alvarenga, C.J.S., Boggiani, P.C., Liu, D.,
660 Santos, R.V. & Brito Neves, B.B., 2006. Chronology of Neoproterozoic
661 ice ages in central Brazil, in Gaucher, C.; Bossi, J., Eds., *Proceedings V*
662 *South American Symposium on Isotope Geology*, Punta del Este,
663 Uruguay, 2006, **1**, 303–306.
- 664 Babinski, M., Boggiani, P.C., Trindade, R.I.F. & Fanning, C.M. 2013.
665 Detrital zircon ages and geochronological constraints on the
666 Neoproterozoic Puga diamictites and associated BIFs in the southern
667 Paraguay Belt, Brazil. *Gondwana Research* **23**, 988–997.
- 668 Babinski, M., McGee, B., Tokashiki, C.C., Tassinari, C.C.G., Saes, G.S. &
669 Pinho, F.E.C. 2018. Comparing two arms of an orogenic belt during
670 Gondwana amalgamation: Age and provenance of the Cuiabá Group,
671 northern Paraguay Belt, Brazil. *Journal of South American Earth*
672 *Sciences* **85**, 6-42.
- 673 Bandeira, J., Nogueira, A.C.R., Petri, S., Riccomini, C., Trindade, R.I.F.,
674 Sial, A.N. & Hidalgo, R.L., 2007. Depósitos Litorâneos Neoproterozóicos
675 do Grupo Alto Paraguai no sudoeste do Cráton Amazônico, região de
676 Mirassol d Oeste, Mato Grosso. *Brazilian Journal of Geology* **37**, 595–
677 606.
- 678 Bandeira, J., McGee, B., Nogueira, A.C.R., Collins, A.S. & Trindade, R.I.F.
679 2012. Closure of the Neoproterozoic Clymene Ocean: Sedimentary and
680 detrital zircon geochronology evidence from the siliciclastic upper Alto
681 Paraguai Group, northern Paraguay Belt, Brazil. *Gondwana Research*
682 **21**, 323–340.
- 683 Barros, M.A.S, Mizusaki, A.M.P, Weska, R.K, Borba, A.W, Chemale J.R.F.
684 & Costa, E.C. 2007. Petrografia, Geoquímica, Análises Isotópicas (Sr,
685 Nd) e Geocronologia Ar-Ar dos Basaltos de Tapirapuã (Tangará da
686 Serra, Mato Grosso, Brasil). *Pesquisas em Geociências* **33**(2), 71 – 77.
687 UFRGS - Instituto de Geociências.
- 688 Bassot, J.P. 1966. Etude géologique du Sénégal oriental et de ses confins
689 guinéo-maliens. *Mémoires Bureau Recherches Géologiques Minières*,
690 Paris **40**, 322.
- 691 Brelaz, L.C. 2012. Paleoambiente dos Calcários e Folhelhos Betuminosos
692 da Formação Guia, Neoproterozóico, Sudoeste do Estado do Mato
693 Grosso. Msc. Essay, UFPA, Belém-PA, 64 p.
- 694 Cordani U. G., Pimentel M. M., Araújo C. E. G. & Fuck R. A. 2013. The
695 Significance of the Transbrasiliiano-Kandi Tectonic Corridor for the

- 696 Amalgamation of West Gondwana. *Brazilian Journal of Geology* **43**(3),
697 583-597.
- 698 Corrêa, J.A., Correia Filho, F.C.L., Scslewski, G.; Neto, C., Cavallon, L.A.,
699 Cerqueira, N.L.S., Nogueira, V.L 1979. Geologia das Regiões Centro e
700 Oeste de Mato Grosso do Sul. Brasília, DNPM. 111 p. (Geologia Básica
701 3).
- 702 Costa, B.S., Silva, C. H. & Costa, A.C.D. 2015. Caracterização estrutural
703 do domínio interno da Faixa Paraguai na região de cangas, porção
704 centro-sul do Estado de Mato Grosso. *Brazilian Journal of Geology*
705 **45**(1), 35-49.
- 706 Chapman J.B., DeCelles P.G. 2015. Foreland basin stratigraphic control on
707 thrust belt Evolution. *GEOLOGY*, v. **43**; no. 7; p. 579–582.
- 708 Dalziel, I.W.D. 1992. On the Organization of American Plates in the
709 Neoproterozoic and the Breakout of Laurentia. *GSA Today* **2**, 237–241.
- 710 DeCelles, P.G. & Giles K.N. 1996. *Foreland Basin Systems*, Basin Res. **8**,
711 105 – 123.
- 712 DeCelles P.G., Robinson D.M. & Zandt G. 2002. Implications of Shortening
713 in the Himalayan Fold-Thrust Belt for Uplift of the Tibetan Plateau.
714 *Tectonics* **21**(6), 1062.
- 715 Delgado A., Mora A., Reyes-Harker A. 2012. Deformation partitioning in
716 the Llanos foreland basin during the Cenozoic and its correlation with
717 mountain building in the hinterland. *Journal of South American Earth*
718 *Sciences* **39**, 228-244.
- 719 Del'Rey Silva L.J.H. 1990. Ouro no Grupo Cuiabá, Mato Grosso: Controles
720 Estruturais e Implicações Tectônicas. In: *Congresso Brasileiro de*
721 *Geologia*, 36. Natal, Annals, **6**, 2520-2534.
- 722 De Min A., Hendriks B., Slejko F., Comin-Chiaramonti P., Girardi V.A.V.,
723 Ruberti E., Gomes C., Neder R.D. & Pinho F.C. 2013. Age of ultramafic-
724 K rocks from Planalto da Serra, Mato Grosso, Brazil. *Journal of South*
725 *American Earth Science* **41**, 57-64.
- 726 De Paola, N., Holdsworth, R.E. & McCaffrey, K.J.W. & Barchi, M.R. 2005.
727 Partitioned transtension: an alternative to basin inversion models.
728 *Journal of Structural Geology*, **27**, 607-625.
- 729 Dewey, J.F., Holdsworth, R.E. & Strachan, R.A. 1998. Transpression and
730 transtension zones. In: Holdsworth, R.E., Strachan, R.A., Dewey, J.F.
731 (Eds.), Continental Transpressional and Transtensional Tectonics.
732 *Geological Society Special Publication* **135**, 1–14.
- 733 Deynoux M., Affaton P., Trompette R. & Villeneuve M. 2006. Pan-African
734 tectonic evolution and glacial events registered in Neoproterozoic to
735 Cambrian cratonic and foreland basins of West Africa. *Journal of African*
736 *Earth Sciences* **46**, 397-426.

- 737 Fossen, H., Tikoff, B. & Teyssier, C. 1994. Strain modeling of
738 transpressional and transtensional deformation. *Norsk Geologisk*
739 *Tidsskrift* **74**, 134-145.
- 740 Fossen, H., Cavalcante, G.C.G., Pinheiro, R.V.L., Archanjo, C.J. 2018.
741 Deformation – Progressive or multiphase?. *Journal of Structural*
742 *Geology*. DOI: 10.1016/j.jsg.2018.05.006.
- 743 Geraldes, M., Tassinari, C., Babinski, M., Martinelli, C., Iyer, S., Barboza,
744 E., Pinho, F. & Onoe, A. 2008. Isotopic evidence for the Late Brasiliano
745 (500–550 Ma) ore-forming mineralization of the Araés Gold Deposit.
746 *Brazil: International Geology Review* **50**, 177–190.
- 747 Hoffman P.F. & Schrag D.P. 2002. The Snowball Earth hypothesis: testing
748 the limits of global change. *Terra Nova* **1**, 129-155.
- 749 Holdsworth, R.E., Tavarnelli, E., Clegg, P., Pinheiro, R.V.L., Jones, R.R. &
750 McCaffrey, K.J.W. 2002. Domainal deformation patterns and strain
751 partitioning during transpression: an example from the Southern
752 Uplands terrane, Scotland. *Journal of the Geological Society*, London,
753 **159**, 401-415.
- 754 Jones, R.R., Holdsworth, R.E., Clegg, P., McCaffrey, K. & Tavarnelli, E.,
755 2004. Inclined Transpression. *Journal of Structural Geology*, **26**, 1531–
756 1548.
- 757 Kirschvink, J.L., Ripperdan, R.L. & Evans, D.A., 1997. Evidence for a
758 large-scale reorganization of early Cambrian continental masses by
759 inertial interchange true polar wander. *Science* **277**, 541–545.
- 760 Luz, J.S., Oliveira, A.M., Souza, J.O., Motta, J.J.I.M., Tanno, L.C., Carmo,
761 L.S., Souza, N.B., 1980. Projeto Coxipó - relatório Final. Companhia de
762 Pesquisa de Recursos Minerais. Superintendência Regional de Goiânia.
763 DNPM CPRM 1, 136.
- 764 Maciel, P. 1959. Tilito Cambriano (?) no Estado de Mato Grosso. *Soc.*
765 *Bras. Geol. Boletim* **8**, 3–49.
- 766 Martinelli C.D. 1998. Petrografia, estrutural e fluidos da mineralização
767 aurífera dos Araés-Nova Xavantina-MT. Ph.D. Thesis, Universidade
768 Estadual Paulista, Rio Claro, 183.
- 769 McGee, B., Collins, A.S., & Trindade, R.I.F. 2012. G'day Gondwana—The
770 final accretion of a supercontinent: U-Pb ages from the post-orogenic
771 São Vicente Granite, northern Paraguay Belt, Brazil. *Gondwana*
772 *Research* **21**, 316–322.
- 773 McGee, B., Collins, A.S., & Trindade, R.I.F., Jourdan, F. 2014.
774 Investigating mid-Ediacaran glaciation and final Gondwana
775 amalgamation using coupled sedimentology and $^{40}\text{Ar}/^{39}\text{Ar}$ detrital
776 muscovite provenance from the Paraguay Belt, Brazil. *Sedimentology*
777 **62**, 130-154.

- 778 McGee, B., Collins, A.S., Trindade, R.I.F. & Payne J. 2015. Age and
779 provenance of the Cryogenian to Cambrian passive margin to foreland
780 basin sequence of the northern Paraguay Belt, Brazil. *Geological Society
781 of America Bulletin*, **127**, n. ½.
- 782 Merdith, A.S., Collins A.S., Williams, S.E., Pisarevsky, S., Foden J.F.,
783 Archibald D., Blades M.L., Alessio B.L., Armistead S., Plavsa D., Clark,
784 C., Müller R.D. 2017. A full-plate global reconstruction of the
785 Neoproterozoic. *Gondwana Research*, Vol. **50**, 84-134.
- 786 Milhomem Neto, J.M., Nogueira, A.C.R, Macambira, M.J.B. 2013. A
787 seção-tipo da Formação Serra do Quilombo, Grupo Araras,
788 Neoproterozoico da Faixa Paraguai Norte, Mato Grosso. *Brazilian
789 Journal of Geology*, 43(2): 385-400.
- 790 Montes-Lauar, C.R., Pacca, I.G., Melfi, A.J., Piccirillo, E.M., Bellieni, G.,
791 Petrine, R. & Rizzieri, R. 1994. The Anari and Tapirapuã Jurassic
792 formations, western Brazil: paleomagnetism, geochemistry and
793 geochronology. *Earth and Planetary Science Letters* **128**, 357-71.
- 794 Mouthereau F., Filleaudeau P.Y., Vacherat, A. Pik R. Lacombe O., Fellin
795 M.G. Castelltort S., Christophoul F. Masini E. 2014. Placing limits to
796 shortening evolution in the Pyrenees: Role of margin architecture and
797 implications for the Iberia/Europe convergence. *Tectonics*, 33.
- 798 Nogueira, V.L & Oliveira, C.C. 1978. Projeto Bonito Aquidauana. Goiânia,
799 DNPM/CPRM. 121 p. (Technical Report).
- 800 Nogueira, A.C.R., Riccomini, C., Sial, A.N., Moura, C.A.V. & Fairchild, T.R.
801 2003. Soft-sediment deformation at the base of the Neoproterozoic
802 Puga cap carbonate (southwestern Amazon craton, Brazil):
803 confirmation of rapid icehouse to greenhouse transition in snowball
804 earth. *Geology* **31**, 613-616.
- 805 Nogueira, A.C.R. & Riccomini, C. 2006. O Grupo Araras (Neoproterozóico)
806 na parte norte da Faixa Paraguai e Sul do Cráton Amazônico, Brasil.
807 *Brazilian Journal of Geology* **36**, 623-640.
- 808 Nogueira A.C.R., Riccomini C., Sial A.N., Moura C.A.V., Trindade R.I.F. &
809 Fairchild T.R. 2007. Carbon and strontium isotope fluctuations and
810 paleoceanographic changes in the late Neoproterozoic Araras carbonate
811 platform, southern Amazon craton, Brazil. *Chemical Geology* **237**, 168-
812 190.
- 813 Nogueira A.C.R., Romero G.R., Sanches E., Domingos F.H.G., Bandeira J.,
814 Santos I.M., Pinheiro R.V.L., Soares J.L., Lafon J.M., Afonso J.W.L.,
815 Santos H.P. & Rudnitzki I.D. 2019. The Cryogenian–Ediacaran Boundary
816 in the Southern Amazon Craton. *Chemostratigraphy Across Major
817 Chronological Boundaries, Geophysical Monograph 240*, First Edition.
818 *AGU Books*.

- 819 Paixão M.A.P, Nilson A.A., Dantas E.L. 2008. The Neoproterozoic
820 Quatipuru ophiolite and the Araguaia fold belt, central-northern Brazil,
821 compared with correlatives in NW Africa In: Pankhurst R. J., Trouw R.
822 A. J., Brito Neves B. B. & De Wit M. J. (eds) West Gondwana: Pre-
823 Cenozoic Correlations Across the South Atlantic Region. *Geological*
824 *Society, London, Special Publications*, 294, 297–318.
- 825 Pires F.R.M., Gonçalves F.T.T., Ribeiro L.A.S. & Siqueira A.J.B. 1986.
826 Controle das mineralizações auríferas do Grupo Cuiabá, Mato Grosso.
827 In: *34 Congresso Brasileiro de Geologia, Goiânia, Annals, SBG, 5,*
828 *2383-2395.*
- 829 Roigé, M., Gómez-Gras, D., Remacha, E., Boya, S., Viaplana-Muzas M.
830 Teixell, A. 2017. Recycling an uplifted early foreland basin fill: An
831 example from the Jaca basin (Southern Pyrenees, Spain). *Sedimentary*
832 *Geology* **360**, 1–21.
- 833 Romero, J.A.S., Lafon, J.M., Nogueira, A.C.R. & Soares, J. L. 2013. Sr
834 isotope geochemistry and Pb-PB geochronology of the Neoproterozoic
835 cap carbonates, Tangará da Serra, Brazil. *Inter. Geo. Rev.* **55**, 1-19.
- 836 Santos, H.P., Mangano, M. G., Soares, J.L., Nogueira, A.C.R., Bandeira,
837 J., & Rudnitzki, I.D. 2017. Ichnologic evidence of a Cambrian age in the
838 Southern Amazon Craton: Implications for the onset of the Western
839 Gondwana history. *Journal of South American Earth Sciences* **76**, 482-
840 488.
- 841 Saura, E., Verge, J., Homke, P., Blanc, E. Serra-Kiel, J., Bernaolas, G.,
842 Casciello, E., Fernandez, N. Romaine, I., Casini, G., Embry, J.C., Sharp,
843 I.R., Hunt, D.W. 2011. Basin architecture and growth folding of the NW
844 Zagros early foreland basin during the Late Cretaceous and early
845 Tertiary. *Journal of the Geological Society, London, Vol. 168*, 2011, pp.
846 235–250.
- 847 Silva, C.H. 1999. Caracterização Estrutural de Mineralizações
848 Auríferas do Grupo Cuiabá, Baixada Cuiabana (MT). Msc. Essay, UNESP,
849 Rio Claro, 134 p.
- 849 Shields, G.A., Deynoux M., Culver S. J., Brasier, M.D., Affaton P. &
850 Vandamme, D. 2007. Neoproterozoic glaciomarine and cap dolostone
851 facies of the southwestern Taoudéni Basin (Walidiala Valley,
852 Senegal/Guinea, NW Africa). *Geoscience* **339**, 186–199.
- 853 Silva, C.G., 1999. Caracterização Estrutural de Mineralizações auríferas do
854 Grupo Cuiabá, Baixada Cuiabana (MT). PhD thesis. Instituto de
855 Geociências e Ciências Exatas da Universidade Estadual Paulista, Rio
856 Claro.
- 857 Silva, C.H., Simões L.S.A. & Ruiz, A.S. 2002. Caracterização Estrutural
858 dos Veios Auríferos da Região de Cuiabá, MT. *Brazilian Journal of*
859 *Geology* **32**(4), 407-418.

- 860 Souza, N.B. 1981. O Grupo Cuiabá na área do Projeto Coxipó.
861 Estratigrafia e potencialidade econômica. In: *SIMP. GEOL. CENTRO-*
862 *OESTE*, SBG. 226-239.
- 863 Tikoff, B. & Fossen, H. 1999. Three-dimensional reference deformations
864 and strain facies. *Journal of Structural Geology* **21**, 1497-1512.
- 865 Tohver, E., Trindade, R.I.F., Riccomini, C., Font, E., 2006. Bending of the
866 Paraguay Belt: the secondary origin of a curved, Cambrian an
867 implication for Gondwanan assembly. In: *Anais do XVIII Congresso*
868 *Brasileiro de Geologia*. Aracajú-SE, p. 186.
- 869 Tohver E., Trindade R.I.F., Solum J.G., Hall C.M., Riccomini C. & Nogueira
870 A.C. 2010. Closing the Clymene ocean and bending a Brasiliano belt:
871 Evidence for the Cambrian formation of Gondwana, southeast Amazon
872 craton. *Geology* **38**, 267-270.
- 873 Tohver, E., Cawood, P.A., Rosello, E.A. & Jourdan, F., 2011. Closure of
874 the Clymene Ocean and formation of West Gondwana in the Cambrian:
875 evidence from the Sierras Australes of the southernmost Rio de la Plata
876 craton, Argentina. *Gondwana Research*, **21**, 394-405.
- 877 Tokashiki, C. C. & Saes, G. S. 2008. Revisão Estratigráfica e Faciológica
878 do Grupo Cuiabá no alinhamento Cangas-Poconé, Baixada Cuiabana,
879 Mato Grosso. *Brazilian Journal of Geology* **38**(4), 661-675.
- 880 Trindade, R.I.F., D'agrella-Filho, M.S., Epof, I., & Brito Neves, B.B. 2006.
881 Paleomagnetism of Early Cambrian Itabaiana mafic dikes (NE Brazil)
882 and the final assembly of Gondwana. *Earth and Planetary Science*
883 *Letters* **244**, 361-377.
- 884 Trompette, R. 1994. Geology of Western Gondwana (2000-500Ma). Pan-
885 African - Brasiliano aggregation of South America and Africa. *Balkema*,
886 **350**.
- 887 Trompette, R., 1997. Neoproterozoic (600 Ma) aggregation of Western
888 Gondwana: a tentative scenario. *Precambrian Research* **82**, 101-112.
- 889 Vasconcelos, B.R., Ruiz A.S. & Matos J.B. 2015. Polyphase deformation
890 and metamorphism of the Cuiabá group in the Poconé region (MT),
891 Paraguay Fold and Thrust Belt: kinematic and tectonic implications.
892 *Brazilian Journal of Geology* **45**(1), 51-63.
- 893 Villeneuve, M., 1982. Schéma lithostratigraphique des Mauritanides au
894 Sud du Sénégal et au Nord de la Guinée d'après les données actuelles.
895 *Bull. Soc. Géol. France*, **7**, 249-254.
- 896 Villeneuve, M., 1984. Etude géologique de la bordure SW du Craton Ouest
897 Africain. Thèse Univ. Aix-Marseille III, 552.
- 898 Villeneuve M. 2005. Paleozoic basins in West Africa and the Mauritanide
899 thrust belt. *Journal of African Earth Sciences* **43**, 166-195.

- 900 Villeneuve M. 2008. Review of the orogenic belts on the western side of
 901 the West African craton: the Bassarides, Rockelides and Mauritanides.
 902 *Geological Society of London, Special Publications* **297**, 169-201.
- 903 Villeneuve, M. & Cornée, J.J. 1994. Structure, evolution and
 904 palaeogeography of the West African craton and bordering belts during
 905 the Neoproterozoic. *Precambrian Research* **69**, 307-326.
- 906 Zhang, Q.H., Ding, L., Cai, F.L., Xu, X.X., Zhang, L.Y., Xu, Q., Willem, H.
 907 2011. Early Cretaceous Gangdese retroarc foreland basin evolution in
 908 the Selin Co basin, central Tibet: evidence from sedimentology and
 909 detrital zircon geochronology. From: Gloaguen, R. & Ratschbacher, L.
 910 (eds) Growth and Collapse of the Tibetan Plateau. *Geological Society,
 911 London, Special Publications*, **353**, 27-44.

912

913

914 **Figure Captions**

915 Fig. 1. Palaeogeographic reconstruction of West Gondwana showing the
 916 central and northeastern parts of the South American platform and
 917 northwestern Africa which assembled during the Brasiliano/Pan-African
 918 Orogeny (adapted from Villeneuve 2008 and Cordani *et al.* 2013).

919 Fig. 2. Tectono-stratigraphic framework of the Northern Paraguai Belt
 920 rocks, according to previous authors (Nogueira *et al.* 2003; Tokashiki &
 921 Saes 2008; Bandeira *et al.* 2012; McGee *et al.* 2012, 2015; Babinski *et al.*
 922 2013, 2018; Santos *et al.* 2017; Nogueira *et al.* 2019).

923 Fig. 3. (A) Structural-geological map of the Northern Paraguai Belt and its
 924 Ediacaran to Early Cambrian cover, and; (B) NW-SE (X-X') cross-section
 925 showing the tectonic arrangement of the rocks and their structural
 926 domains. The locations of Figs 6, 12 and 13 are also shown, as are the
 927 locations of the contraction- and wrench-dominated transpression sub-
 928 domains in the TPSD.

929 Fig. 4. Cuiabá Group lithologies in the field (A) bedded metapelite, (B)
930 phyllite, (C) conglomeratic metasandstone, (D) metasandstones and
931 metapelites with bedding and cleavage, (E) sinistral shear bands and drag
932 folds in metasandstone and (F) stretching lineation in fine continuous
933 foliation in metapelites.

934 Fig. 5. Stereonets of structural data from the metasedimentary rocks of
935 Cuiabá Group. (A) Poles to bedding showing partial girdle related to the
936 development of moderately reclined folds, with NE-SW axial planes and a
937 regional beta axis plunging shallowly SW. (B) Generally NE-SW trending
938 fine continuous foliation showing girdle pattern with beta axis plunging
939 gently NE. (C) NE-SW oblique-thrust faults with stretching lineations
940 plunging gently N, NE and NW. (D) Generally NE-SW trending mylonitic
941 foliation with moderate to high dip angles mainly towards the NW. (E)
942 Gently NE or SW plunging stretching lineations associated with mylonitic
943 foliation. The subdivision into the two domains A and B is based on the
944 difference in strain intensity and lineation strikes. It is suggested that
945 domain B is the product of a wrench dominated transpressional
946 deformation.

947 Fig. 6. Structural cross-sections of structures in key outcrops in the
948 Cuiabá Group. (A) Metasandstone in the TPSD-A domain showing reclined
949 to recumbent folds, associated with a NE-SW sub-horizontal oblique
950 thrust-fault pervasively cut by later NNE-SSW normal fault sets. (B)
951 metapelites in the TPSD-A showing NE-SW foliation cross-cut by NE-SW
952 and NW-SE normal faults. (C) mylonitic phyllonites in the TPSD-B domain

953 with an ENE-WSW fine continuous foliation and sinistral NE-SW sub-
954 vertical shear bands, cut by NW-SE and NE-SW sub-vertical sets of
955 normal faults. For locations of outcrops see Fig. 3. Both the rocks of
956 sections (B) and (C) also preserve syn- to late-kinematic quartz veins.

957 Fig. 7. Photomicrographs of rocks of the Cuiabá Group. (A) and (B) show
958 fine grained metapelites with a spaced foliation defined by the alignment
959 of micas and lenticular polycrystalline quartz grain aggregates with slight
960 sinistral asymmetry.

961 Fig. 8. (A) Metapelites of the Cuiabá Group showing NE-SW zonal
962 crenulation cleavage affecting the older fine continuous fabric with dextral
963 kinematic. (B) photomicrography of fine grained phyllite exhibiting fine
964 continuous fabric deformed by dextrally verging crenulation cleavage.

965 Fig. 9. (A) Pole to planes of NE-SW, NW-SE, N-S and E-W crenulation
966 cleavage with steep to sub-vertical dips towards the SE, NW, SW and N;
967 note that generally NE-SW strikes are dominant. (B) ENE-WSW, NE-SW
968 and NE-SW normal oblique faults with steep to moderate dips towards the
969 N, S, SW and NE to sub-vertical. (C) sub-vertical NW-SE, NE-SW and E-W
970 trending quartz veins in the Cuiabá Group rocks.

971 Fig. 10. Sedimentary rocks exposed in the northern and western portion
972 of the Northern Paraguai Belt: (A) diamictite of the Puga Formation. (B)
973 Cap dolostones of the Mirassol d'Oeste Formation. (C) Calcitic limestones
974 of the Guia Formation. (D) Dolostones of the Nobres Formation. (E)
975 sandstones of the Raizama Formation. (F) Shales of the Diamantino

976 Formation. In all cases note the dominance of bedding and lack of
977 pervasive ductile deformation fabrics.

978 Fig. 11. (A), (F) and (K) Stereonets of poles to bedding in the
979 sedimentary rocks of the Transtensional Structural Domain (TTSD) with
980 general NE-SW strike and gentle to steep or sub-vertical dips towards the
981 NW and SE, for the Cáceres, Nobres and Planalto da Serra areas,
982 respectively (for location, see Fig 3). The observed girdles are related to
983 upright to moderately inclined brittle drag folds, with NE-SW and NW-SE
984 striking axial planes (B, G and L) and (H and M) hinges with moderate to
985 gentle plunges towards the ENE, SE and SW. (C, I and N) NE-SW, NW-SE
986 and N-S normal oblique faults and E-W sub-vertical faults, (D, J and O)
987 with gentle to moderately plunging slickensides towards NW, N, NE, SW
988 and SW. (E) Cataclastic foliations that cross-cut older ductile structures in
989 the Northern Paraguai Belt rocks, with sub-vertical NE-SW and NW-SE
990 strikes.

991 Fig. 12. (A), (B) and (C) Cross-sections in dolomites of the Serra do
992 Quilombo Formation and sandstones of the Raizama Formation (for
993 locations see Fig. 3) showing NE-SW and ENE-WSW striking bedding,
994 locally cut by N-S, NNW-SSE, NE-SW and ENE-WSW sub-vertical normal
995 oblique fault zones, rotating the bedding plane and forming forced drag
996 folds.

997 Fig. 13. (A) Geological map and (B) cross-section of the contact region
998 between de metasedimentary rocks of the Cuiabá Group with calcitic
999 limestones of the Guia Formation, Mina da Brita, NW of N. S. da Guia city

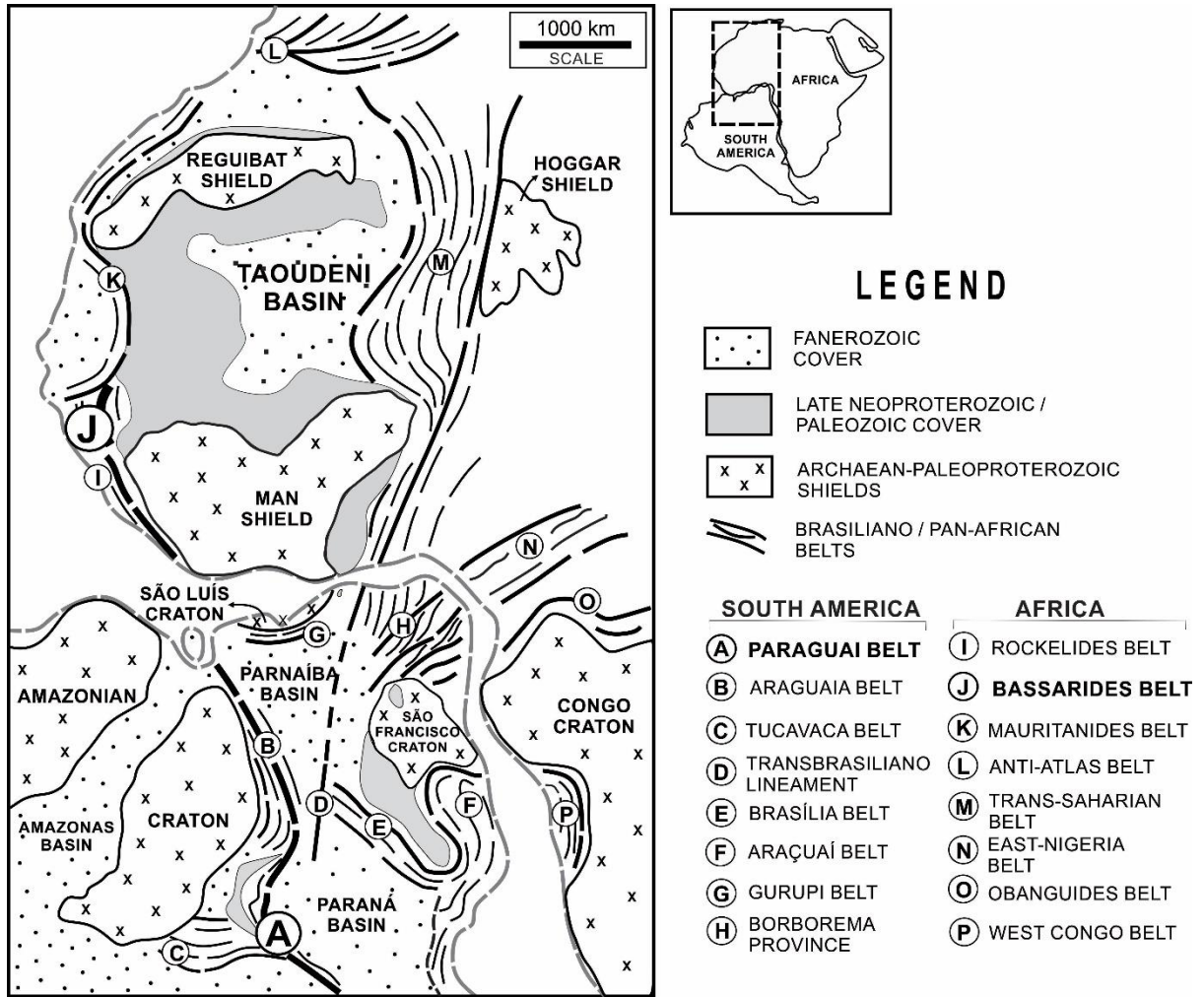
1000 (see Fig. 3 for location). The contact is defined by a NE-SW normal
1001 oblique fault. The Cuiabá Group rocks are steeply dipping and the
1002 limestones are deformed by drag folds related to dextral oblique normal
1003 faulting.

1004 Fig. 14. Tectonic contact between metapelites of the Cuiabá Group with
1005 NE-SW trending fine continuous foliation (to the right) and NE-SW
1006 trending beds of the calcitic limestones of the Guia Formation (to the left),
1007 observed in the Mina da Brita (see Fig. 13). A regional NE-SW normal
1008 oblique fault cuts both the foliation of the metasedimentary rocks and the
1009 beds of the sedimentary sequence, forming an asymmetrical drag or
1010 forced synformal fold.

1011 Fig. 15. (A) Stratigraphic summary of the Northern Paraguai fold and
1012 thrust Belt and Late Cryogenian to Cambrian sedimentary cover (adapted
1013 from Nogueira & Riccomini 2006; Bandeira *et al.* 2012; Alvarenga *et al.*
1014 2012; Santos *et al.* 2017; Nogueira *et al.* 2019). (B) Stratigraphic
1015 sequence summary for the Bassarides Belt and Taoudéni Basin in Africa
1016 (adapted from Trompette 1973; Villeneuve 2005, 2008; Deynoux *et al.*
1017 2006).

1018 Fig. 16. Summary sequence showing the main tectonic episodes proposed
1019 for the regional development for the Northern Paraguai fold and thrust
1020 Belt and subsequent Ediacaran-Early intracratonic basin. (A) Rifting of
1021 Rodinia Supercontinent and establishment of oceanic basin in which the
1022 protoliths of the Cuiabá Group were deposited. (B) Brasiliano/Pan-African
1023 Orogeny including greenschist metamorphism and ductile sinistral

1024 partitioned transpressional deformation verging towards the SE. (C) Uplift
1025 and erosion of the orogen and post-glacial transgression succeeded by the
1026 development of an intracratonic basin, thermal subsidence and late
1027 intrusion of the São Vicente Granite (ca. 518 Ma). (D) Brittle deformation,
1028 dextral oblique normal faulting and forced drag folding in the sedimentary
1029 rocks and brittle overprinting in the underlying basement of the Cuiabá
1030 Group and (E) Younger rift basin development including Mesozoic opening
1031 of the S Atlantic.

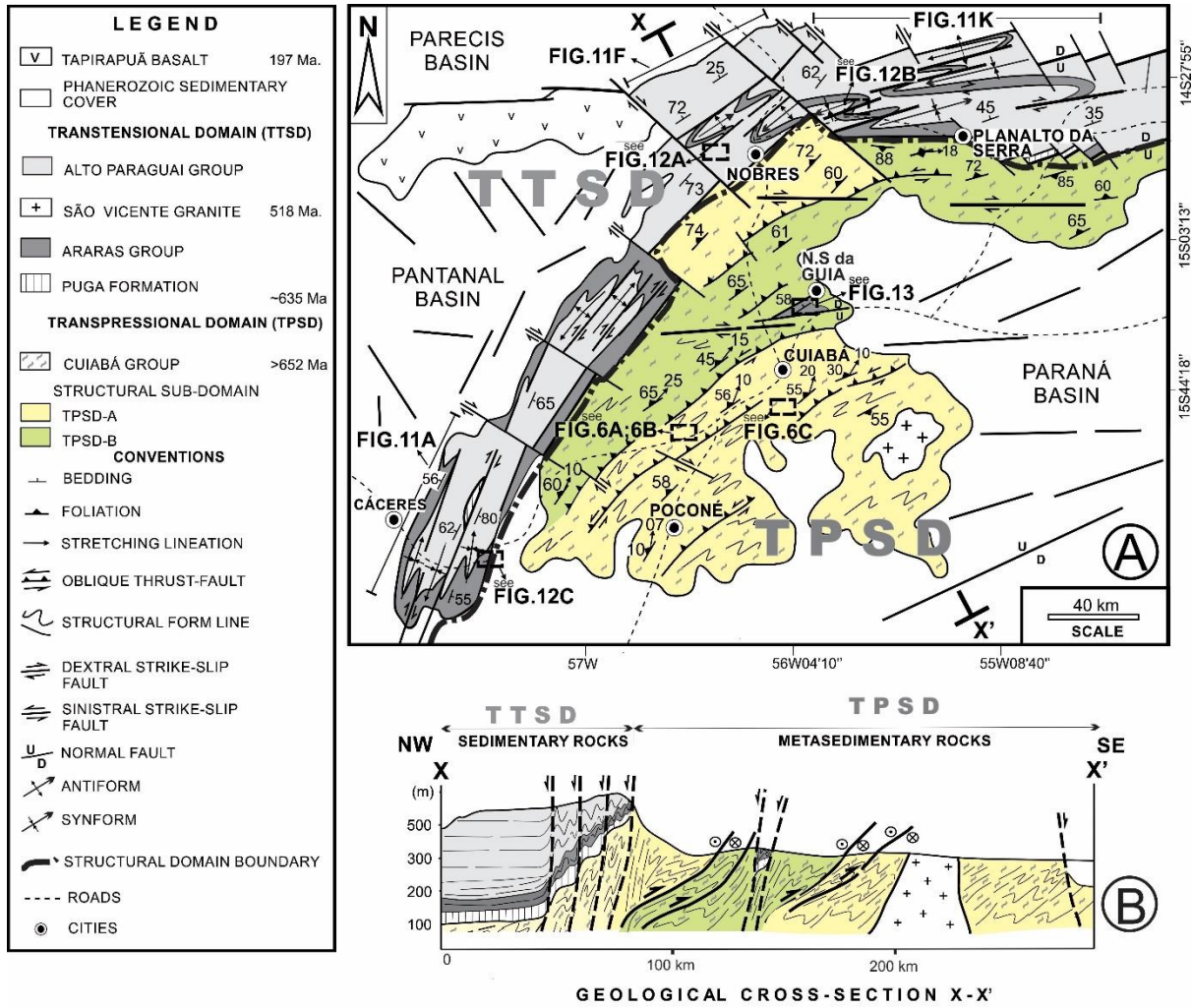


2 Fig. 1.

AGE		MAIN EVENTS	STRATIGRAPHIC UNITS
			CENOZOIC COVER
MESOZOIC	JURASSIC	OPENING OF ATLANTIC OCEAN 197 Ma	TAPIRAPUÃ BASALT SEDIMENTARY COVER (e.g. BAURU BASIN)
PALAEOZOIC	ORDOVICIAN		PALEOZOIC SEDIMENTARY COVER (PARANÁ AND PARECIS BASINS)
	CAMBRIAN	485 Ma GRANITE INTRUSION 518 Ma	ALTO PARAGUAI GROUP DIAMANTINO FORMATION → Fig.10F SE POTUBA FORMATION RAIZAMA FORMATION → Fig.10E
NEOPROTEROZOIC	EDIACARAN	541 Ma	80 Ma
	LATE- CRYOGENIAN	MARINOAN TILLITE 635 Ma	ARARAS GROUP NOBRES FORMATION → Fig.10D SERRA DO QUILOMBO FORMATION GUIA FORMATION → Fig.10C MIRASSOL D'OESTE FORMATION → Fig.10B
	TONJIAN/ EARLY-CRYOGENIAN	BRASILIANO OROGENY PARAGUAI BELT >652 Ma	PUGA FORMATION → Fig.10A CUIABÁ GROUP Fig.4
		RIFTING OF RODINIA	
PALAEO/ MESOPROTEROZOIC		2.1 Ga	AMAZONIAN CRATON (BASEMENT)

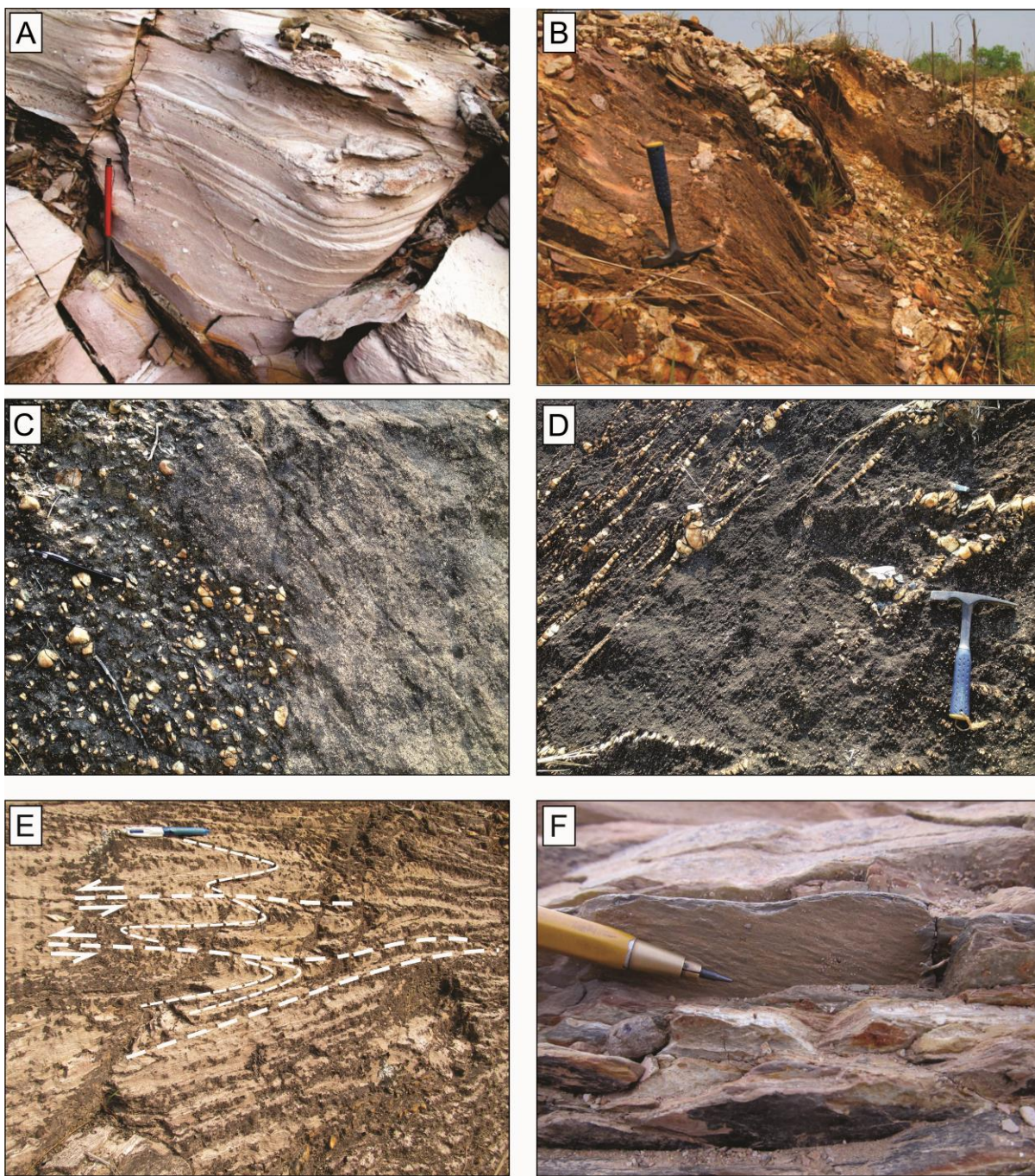
3

4 Fig. 2.



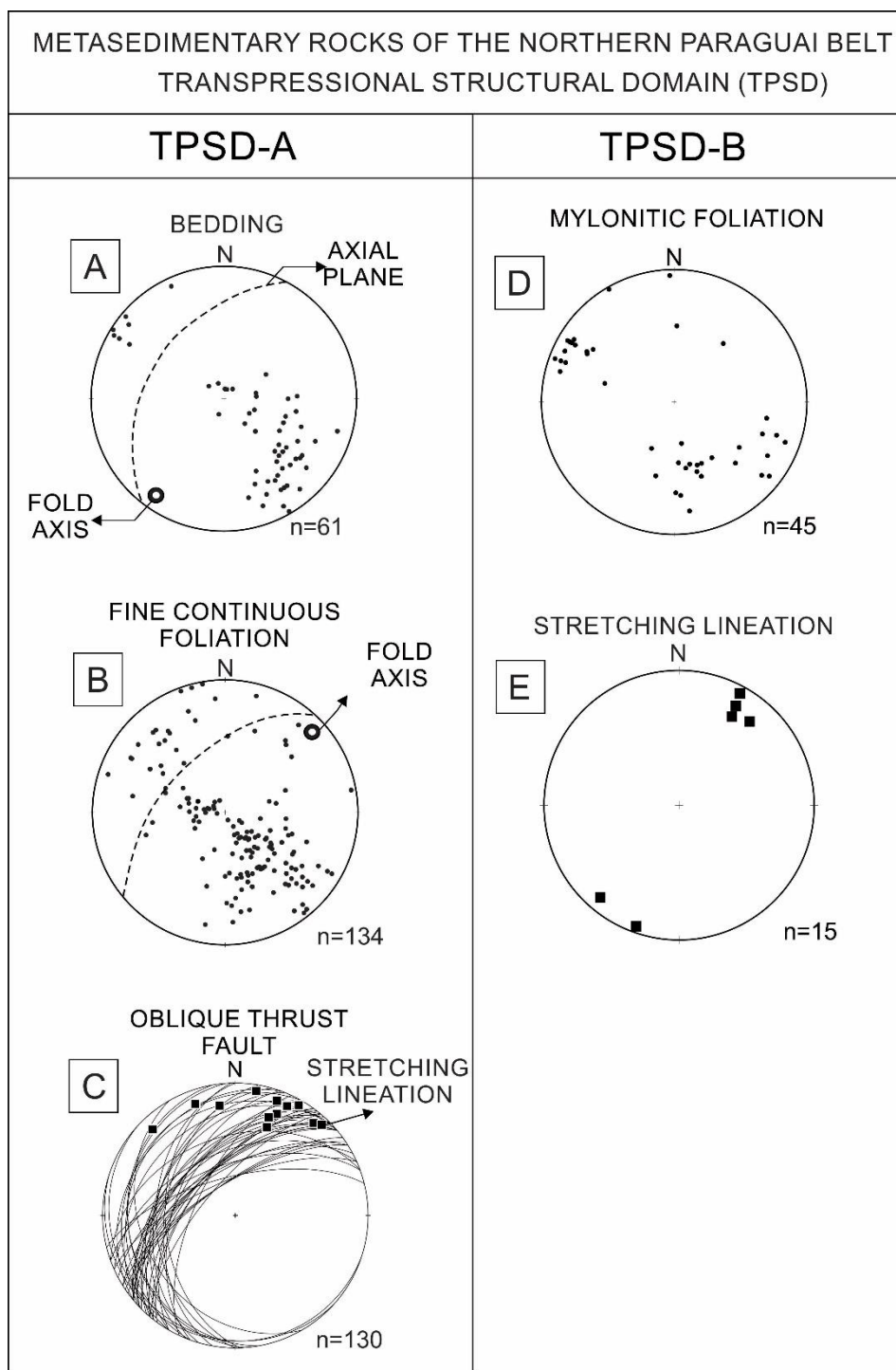
5

6 Fig. 3.



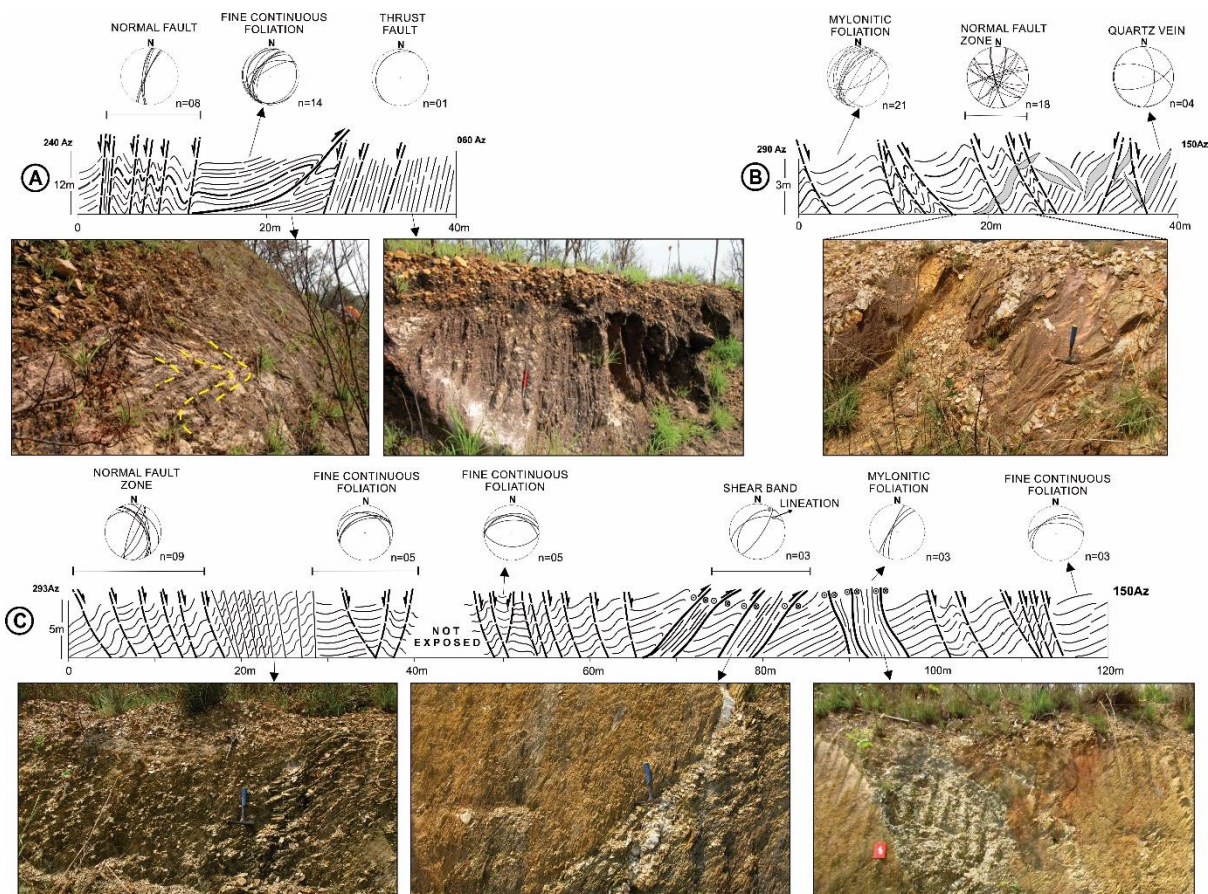
7

8 Fig. 4.



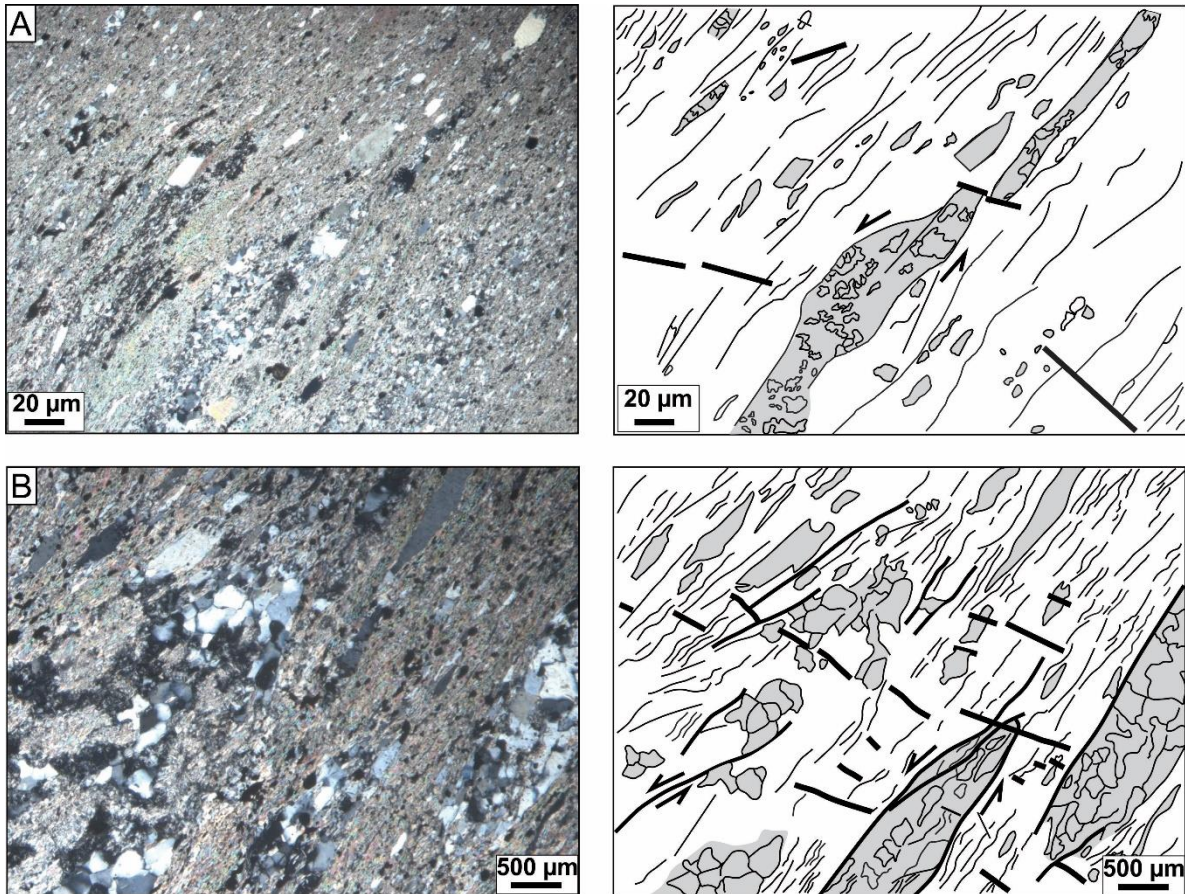
9

10 Fig. 5.



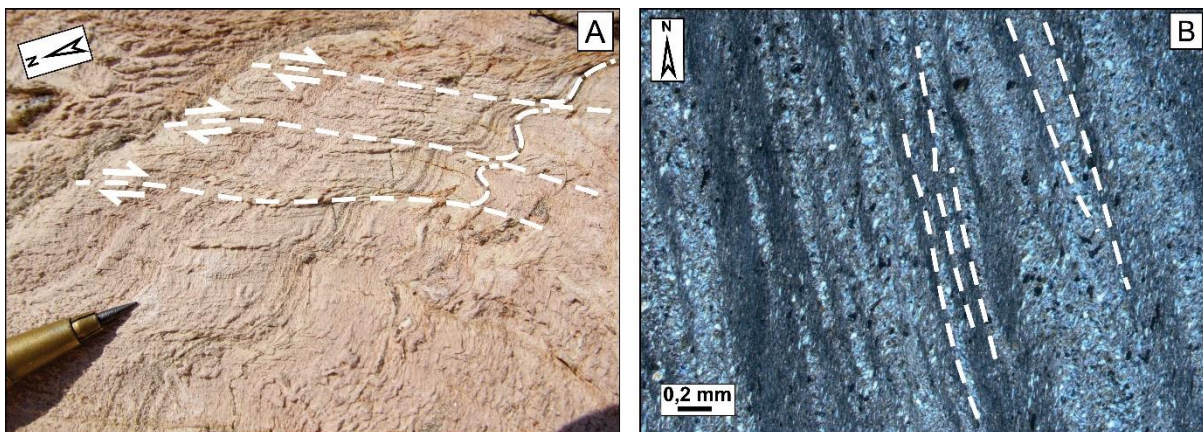
11

12 Fig. 6.



13

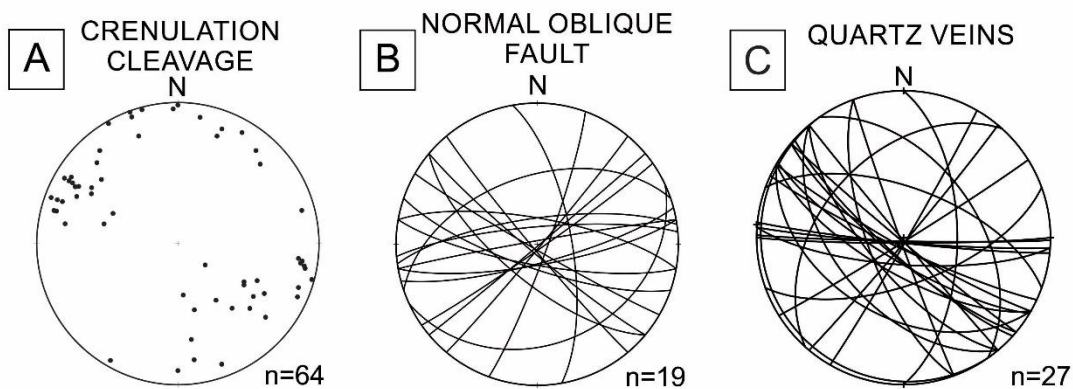
14 Fig. 7.



15

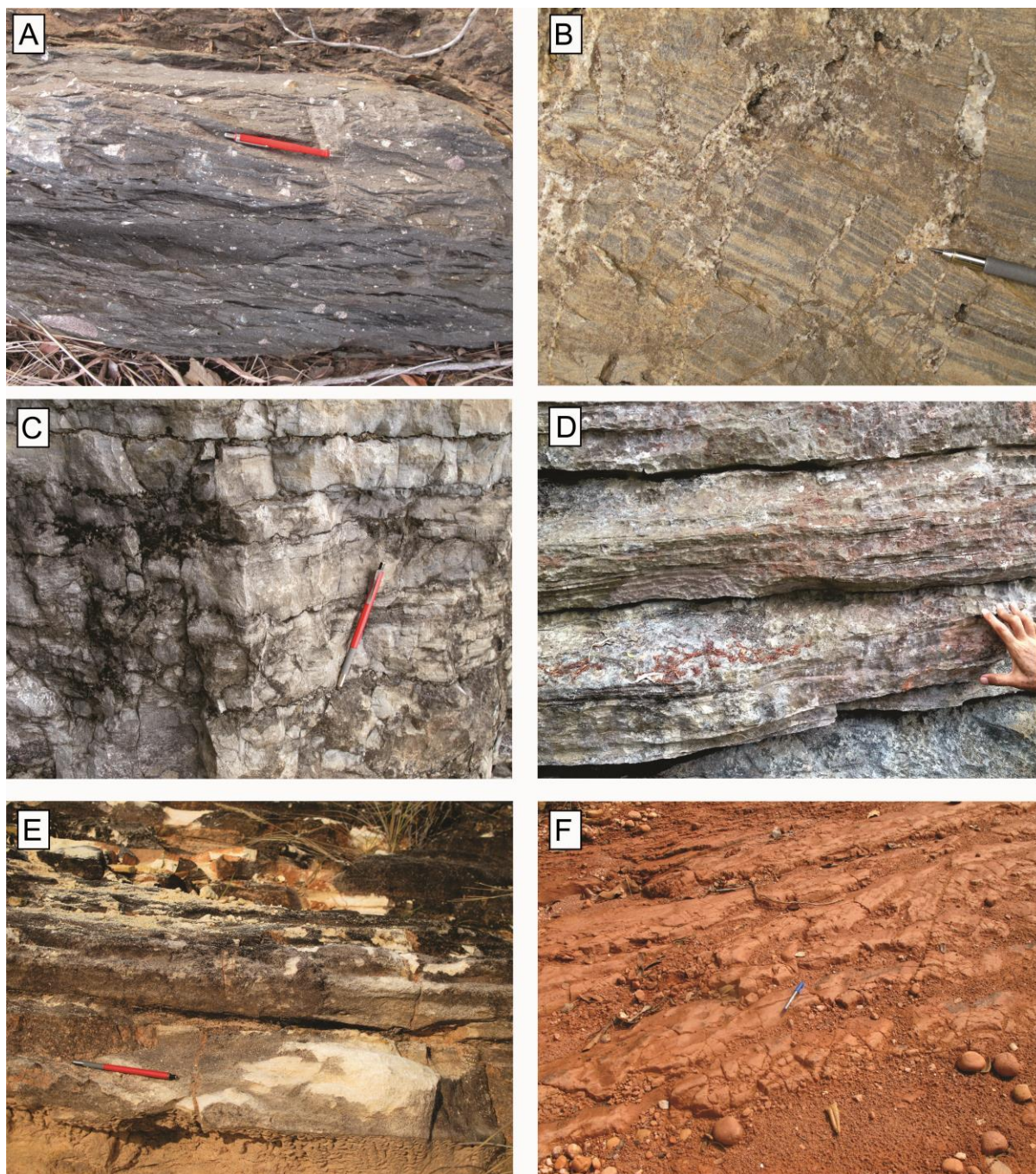
16 Fig. 8.

METASEDIMENTARY ROCKS OF THE NORTHERN PARAGUAI BELT
TRANSTENSIONAL STRUCTURAL DOMAIN (TTSD)



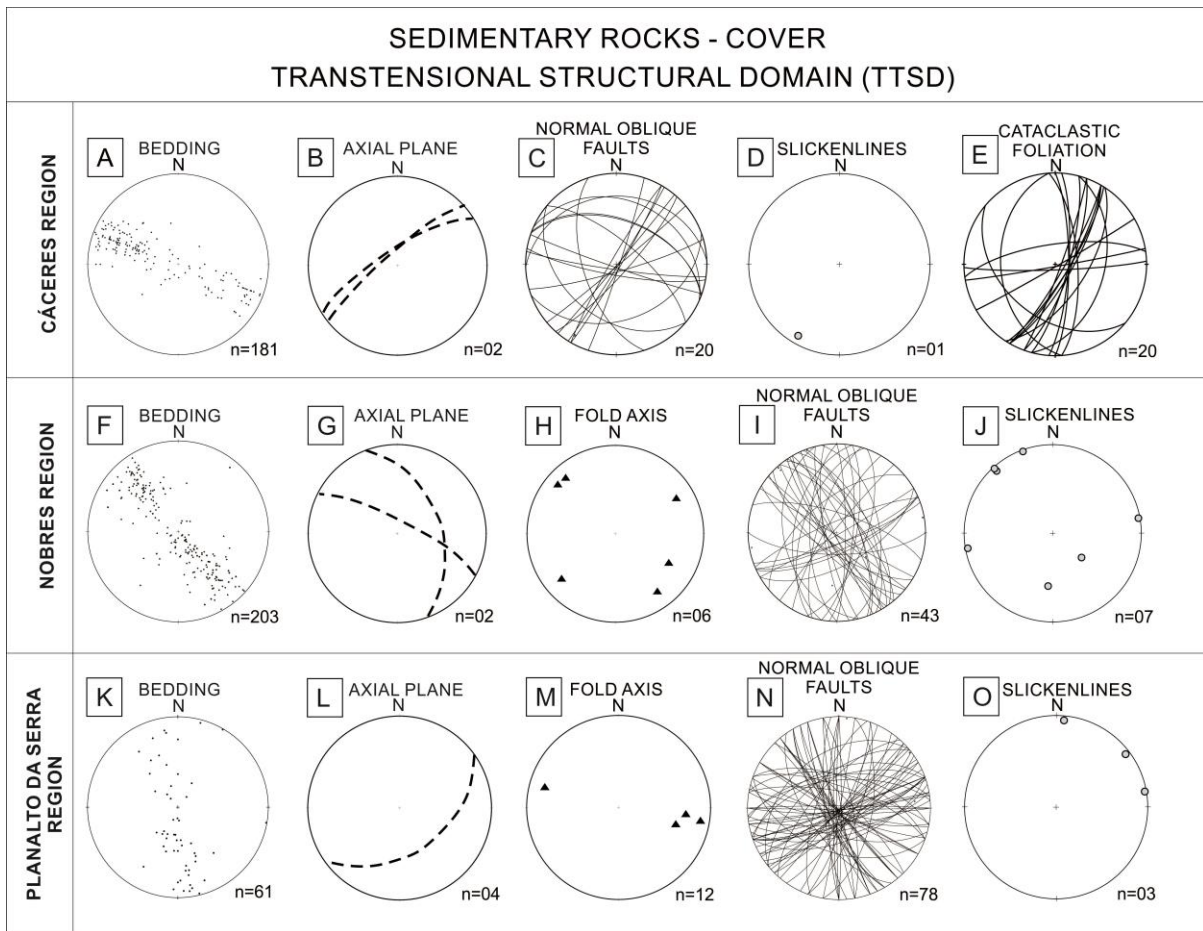
17

18 Fig. 9.



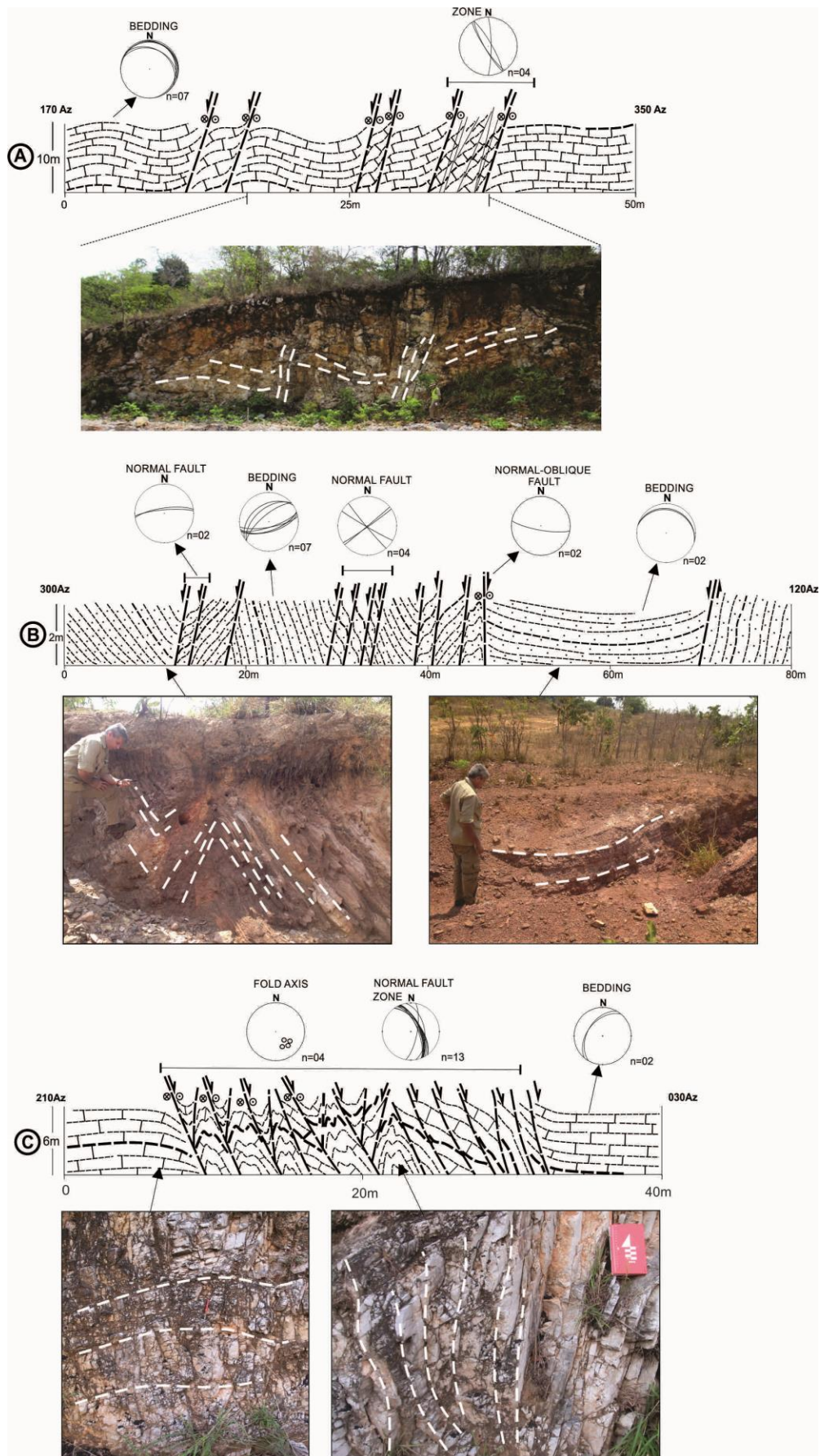
19

20 Fig. 10.



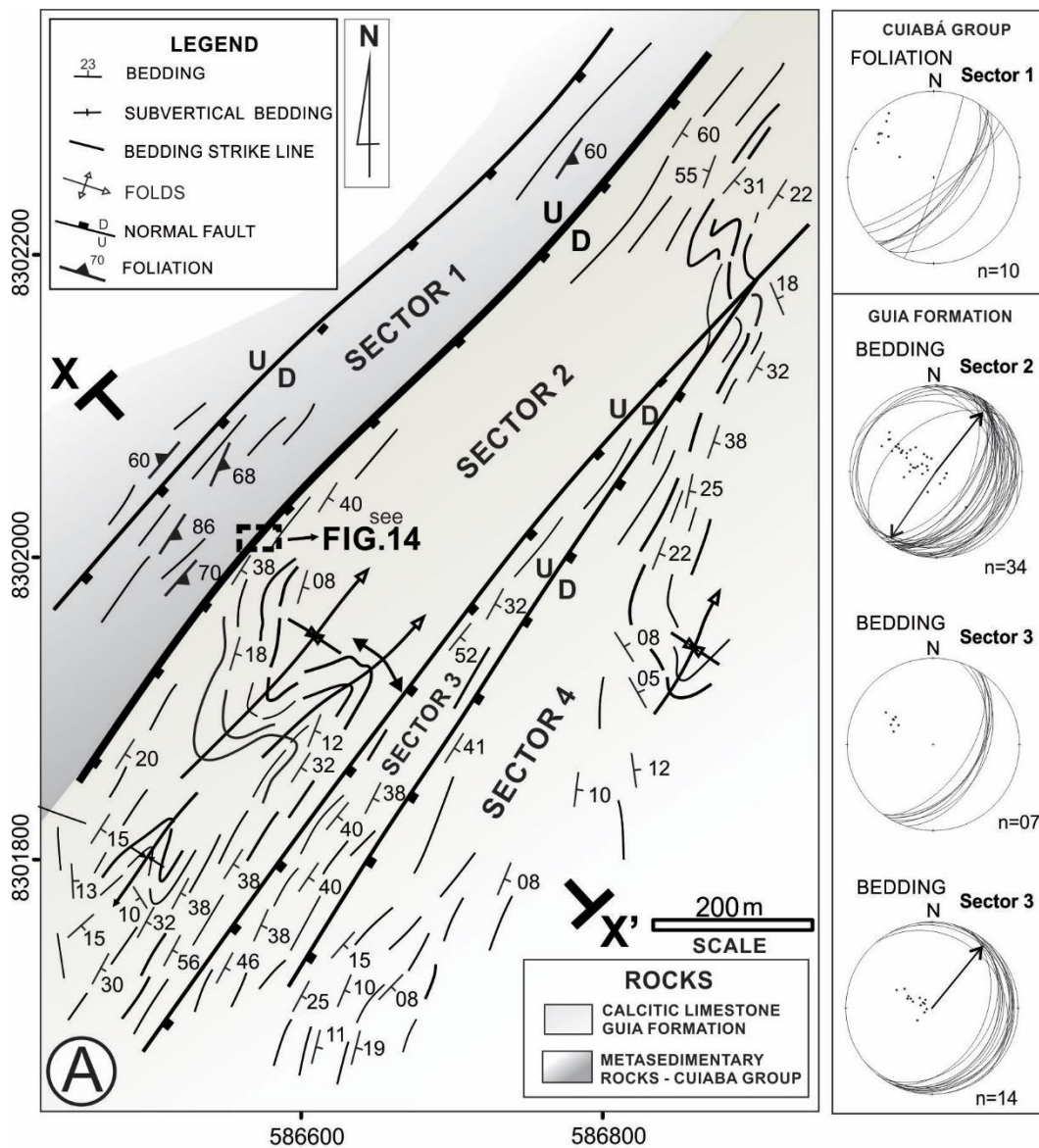
21

22 Fig. 11.



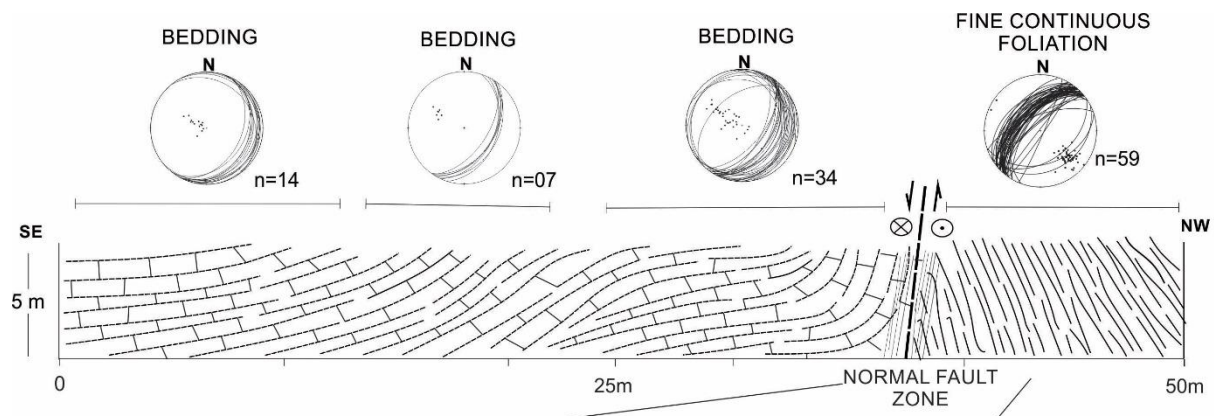
23

24 Fig. 12.



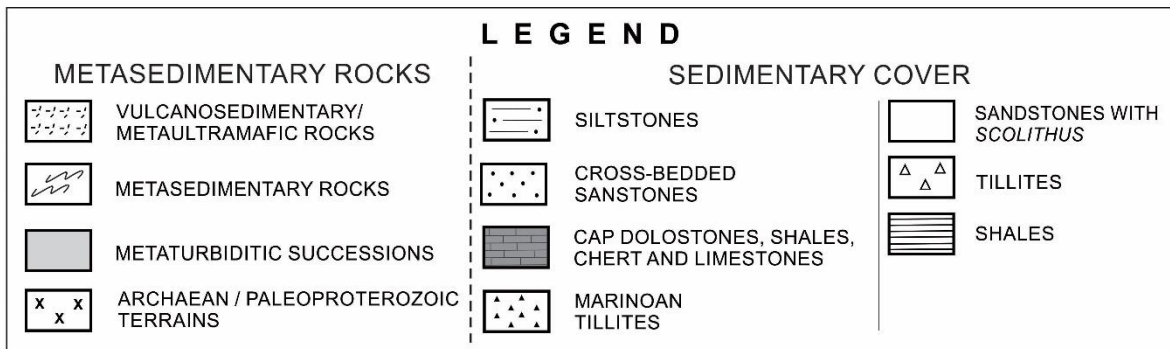
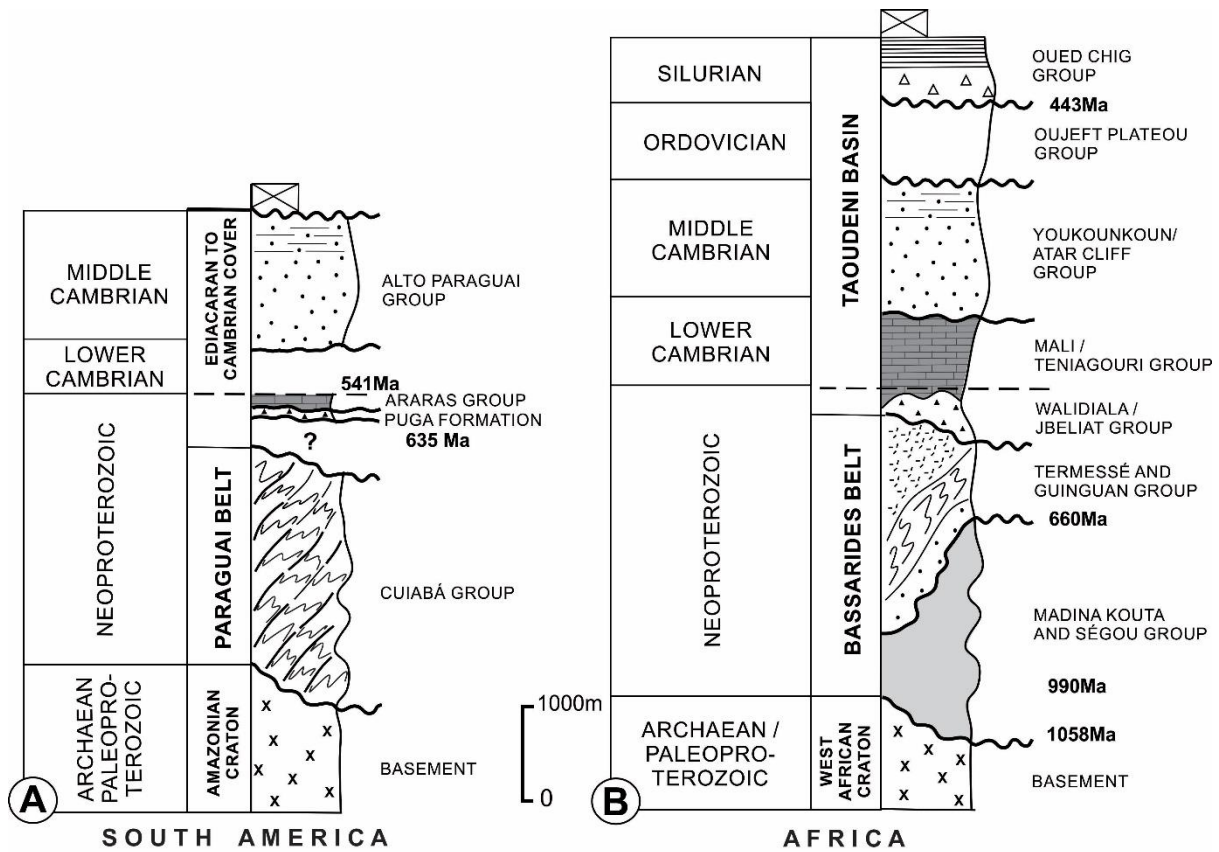
25

26 Fig. 13.



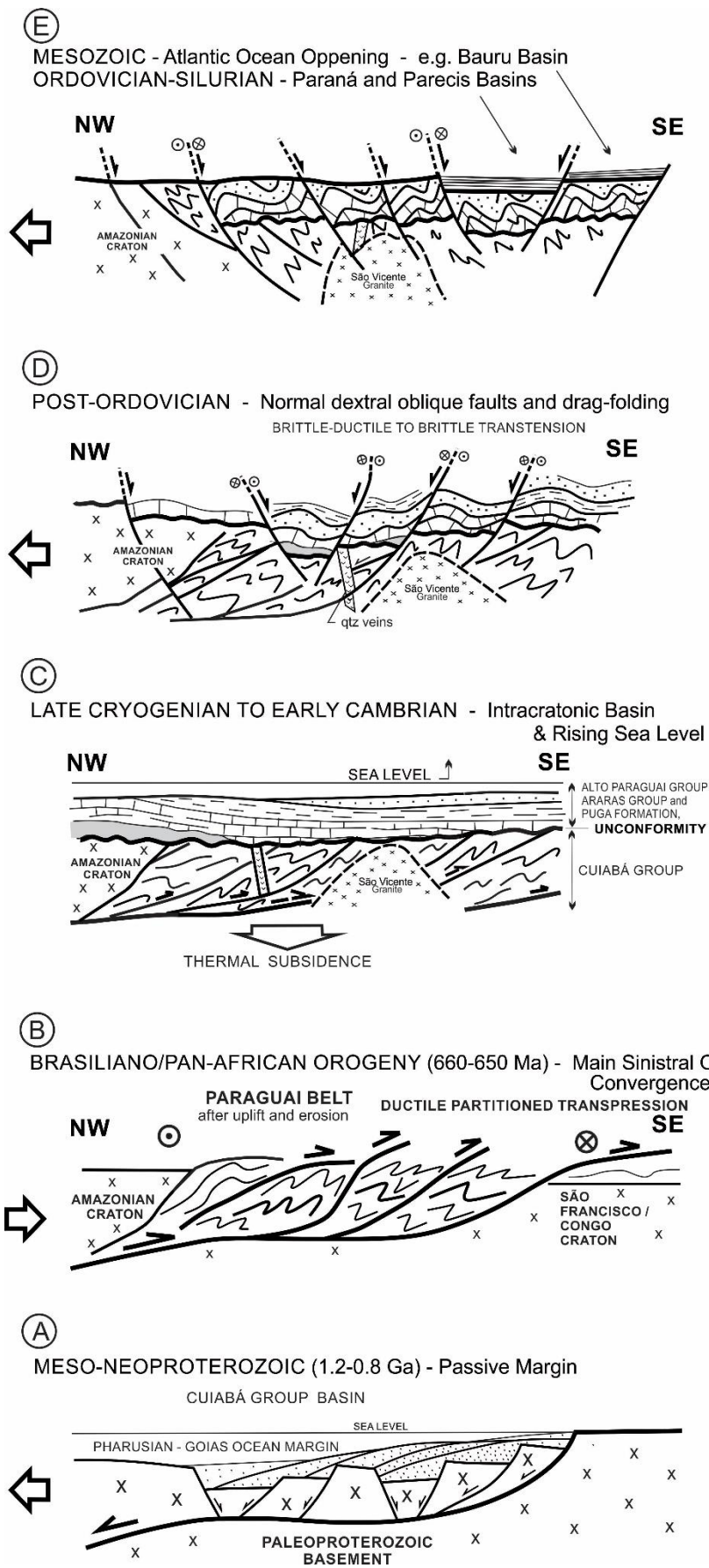
27

28 Fig. 14.



29

30 Fig. 15.



31

32 Fig. 16.